Gene Regulation in the Shipworm Symbiont, *Teredinibacter turnerae* Strain T7901

Brian Scott Fishman
B.S., Indiana University, 2005

Presented to the Division of Environmental & Biomolecular Systems within
The Department of Science & Engineering
and the Oregon Health & Science University
School of Medicine
in partial fulfillment of
the requirements for the degree of
Master of Science
in
Biochemistry and Molecular Biology

June 2010

Department of Science & Engineering

School of Medicine

Oregon Health & Science University

CERTIFICATE OF APPROVAL

This is to certify that the Master's thesis of

Brian Scott Fishman

has been approved

Dr. Margo G. Haygood
Thesis Research Advisor
Professor

Dr. Jorge Crosa
Professor
Department of Molecular Microbiology and Immunology

Dr. Kati Geszvain
Senior Research Associate
Department of Science and Engineering

Dedicated to My Parents, Bernie and Janice, Who Inspire Me to Live Each Day without Limits

Acknowledgement

It was my pleasure and honor to perform this work under the expert guidance of my research advisor, Dr. Haygood. Throughout my work in Dr. Haygood's laboratory, she has embraced my scientific creativity and provided me with the advice and resources that allowed me to reach my goals. In doing so, this opportunity has allowed me to flourish intellectually, as well as individually.

I am also grateful for the technical advice and assistance that I received from all of the Haygood and Tebo lab members. Thanks to Dan Distel (Ocean Genome Legacy) for his collaborations and for providing shipworm specimens used in this work, and Amaro Trindade-Silva (Federal University of Rio de Janeiro) for his helpful insight throughout all of our discussions. This work was truly a cooperative effort, and would not have been possible without the contributions of these individuals.

My greatest gratitude must also be extended to my friends and family for their continued love and support.

Table of Contents

Acknowledgement v
List of Tables viii
List of Figures ix
Abstract xi

Chapter 1. Introduction to the Teredinid Shipworm Symbiosis 1

Chapter 2. Aim of Research 8

Chapter 3. *T. turnerae* Transcriptome Analysis by Microarray 10
Materials and Methods 13
Results and Discussion 18
Differential expression in response to iron starvation 24
Differential expression in response to phosphate starvation 27
Expression in a cellulosic growth medium 30

Chapter 4. Expression Analysis of Secondary Metabolite Genes by Quantitative Reverse Transcription PCR 33
Materials and Methods 34
Results and Discussion 36

Chapter 5. Isolation, Identification, and Relative Quantitation of *T. turnerae* Outer Membrane Proteins 38
Materials and Methods 38
Results and Discussion 41

Chapter 6. Assays for Bioactive Metabolites in *T. turnerae* Culture Extracts and Identification of Potential Fungal Targets 45
Materials and Methods 47
Results and Discussion 49

Chapter 7. Conclusions.....55

Appendix A. An Alternative Growth Medium for *T. turnerae* Results in Significant Physiological Changes 58

References.....66

Biographical Sketch.....80

List of Tables

1.1 Comparison of carbohydrate-active proteins found in *T. turnerae* and *S. degradans* genomes 4

3.1 Description of *T. turnerae* culture conditions used for microarray analysis 15

3.2 Gene categories with increased probe coverage in microarray chip design 17

4.1 Description of primers used for quantitative reverse transcription PCR analysis of secondary metabolite genes.....34

List of Figures

1.1 Depiction of shipworm anatomy....2
1.2 Plant primary cell wall and enzymatic hydrolysis of cellulose....3
1.3 Specific substrates of *T. turnerae* glycoside hydrolase domains....4
1.4 Nine predicted secondary metabolite gene clusters in the genome of *T. turnerae* T7901....6
3.1 Principle of the chrome azurol S reaction....15
3.2 Growth curves of *T. turnerae* in media with different iron and phosphate concentrations....20
3.3 Relative siderophore activity of iron-replete and iron-limited *T. turnerae* supernatants....21
3.4 Electropherograms of RNA used for expression analysis....23
3.5 Relative expression of region 7 secondary metabolite genes....25
3.6 Relative expression of TonB-dependent receptors....26
3.7 Relative expression of secondary metabolite genes in P_i-limited conditions....28
3.8 Model of a hypothetical type VI secretion system....29
3.9 Relative expression of carbohydrate-active genes in a cellulosic medium....30
3.10 Expression comparison of duplicate reference group hybridizations....32
4.1 Genomic positions of secondary metabolite gene clusters 1, 2, and 7 that were targeted for qRT-PCR....34
4.2 Results of qRT-PCR expression analysis of secondary metabolite genes....37
5.1 SDS-PAGE analysis of outer membrane proteins....42
5.2 Relative quantitation of OM proteins from iron-replete and iron-limited cultures by LC-MS/MS....43
6.1 Disc diffusion bioassays showing antimicrobial activity....45
6.2 Model of fungal growth inhibition imposed by secondary metabolites produced by the shipworm symbiont community....46
6.3 Depiction of a positive antimicrobial bioassay by co-plating technique....49
6.4 Disc diffusion bioassay of phosphate-limited culture extract....50
6.5 Phylogenetic analysis and bioassays of fungal isolates....53

A.1 Depiction of a morphological transition of *T. turnerae* 60
A.2 Relative siderophore activity in SBM and ABM 61
A.3 Expression comparison of secondary metabolite genes in ABM and SBM 62
A.4 Use of an acid-free substrate as a carbon source 63
A.5 Comparison of the growth kinetics of *T. turnerae* SBM and ABM 65

Abstract

Gene Regulation in the Shipworm Symbiont, *Teredinibacter turnerae* Strain T7901

Brian Fishman, B.S.

Master of Science
Division of Environmental and Biomolecular Systems within
The Department of Science & Engineering
and the Oregon Health & Science University
School of Medicine

June 2010

Thesis Advisor: Margo G. Haygood

Natural products are the most valuable source for the discovery and development of new drugs, and have played a pivotal role throughout the history of medicine. The emergence of new diseases and evolution of pathogens has created a dire need for the discovery of new drug classes. *Teredinibacter turnerae* strain T7901, a bacterial symbiont of shipworms, devotes a significant proportion of its genome to the biosynthesis of complex secondary metabolites, and holds the promise of finding novel bioactive metabolites within its genetic potential. These secondary metabolites could function as a chemical defense mechanism in the context of the symbiosis, and their biological activities are likely to be of pharmaceutical relevance as well. This symbiont also has an important nutritional role, by providing its host with the enzymes that facilitate complex polysaccharide degradation. These enzymes are highly tuned to

specifically degrade the primary constituents of woody plant cell walls, and are of interest for the development of biofuel applications.

The present study used microarray and quantitative reverse transcription PCR expression analyses to characterize regulation systems of the secondary metabolite and carbohydrate-active genes in the *T. turnerae* genome. Bioassays were used to characterize the properties of some of the antimicrobial secondary metabolites, as well as the organisms that show susceptibility to them. Collectively, these analyses show that the biosynthesis of an antibacterial molecule and catecholate-like siderophore are regulated by phosphate and iron availability, respectively, and provide evidence for which gene clusters are responsible for their biosyntheses. Outer membrane protein analysis provides additional evidence of the proteins responsible for ferric-siderophore uptake in *T. turnerae*. Microarray expression analysis of the carbohydrate-active genes shows that many are highly expressed, even in the absence of substrate.

The results from this study support the notion that the symbiont plays a crucial nutritional role in the symbiosis, and suggest a novel role in chemical defense against competing microbes. Furthermore, this study has optimized conditions for production of secondary metabolites and cellulolytic enzymes to facilitate future discovery and development of biotechnological applications.

Chapter 1

Introduction to the Teredinid Shipworm Symbiosis

Ecological niche and significance of teredinid shipworms

Wood boring marine bivalves of the family Teredinidae (shipworms) have gained much infamy due to the extensive damage they inflict upon wooden marine structures as a result of their xylotrophy (wood eating). The physiological and morphological diversity of shipworms has allowed them to inhabit estuarine and marine ecosystems worldwide, and tolerate a broad range of salinity, temperature, and oxygen concentration (Distel, 2002), resulting in millions of dollars of damage annually (Sipe *et al.,* 2000). While the availability, affordability, and durability of wood make it a favorable material for marine construction, the ubiquity of shipworms strongly deters the use of wood for this purpose.

Shipworms present a highly modified body plan relative to more typical bivalves, with an elongated physique and reduced shell adapted for mechanical wood boring (Figure 1.1). Shipworms utilize their unconventional shell much like a drill to grind and excavate wood, creating a burrow in which they reside. The shipworm deposits a calcareous lining along the walls of the burrow, strengthening its abode, which opens to the external environment only at the site of entry in the wood. The shipworm can use its pallets to seal off this hole during tidal fluctuations or other adverse environmental circumstances, possibly contributing to its resiliency and perseverance.

The proposed role of the bacterial community inhabiting shipworm gill tissue

Remarkably, the shipworm is able to utilize the excavated wood as its primary carbon source for growth and reproduction. While some shipworm species may

supplement their xylotrophic diet with filter feeding, they are the only marine invertebrates known to exist on a diet consisting predominantly of wood (Gallager *et al.,* 1981). In fact, utilization of wood as a primary food source is relatively rare in the animal kingdom, and in the few instances of this phenomenon, the cellulolytic enzymes are believed to be derived from symbiotic microbes typically found in the gastrointestinal tract of the host (Breznak & Brune, 1994). Lignocellulosic material is amongst the most abundant form of biomass on earth, and such cellulolytic microbes play a significant role in the decomposition side of the carbon cycle (Ohkuma, 2003). In the case of the shipworm, the symbionts are localized to bacteriocytes found within the host's gill tissue, which often encompasses nearly the entire length of the animal (Figure 1.1.B). The exact mechanism by which the symbionts facilitate degradation of wood within the host is presently unclear, and intriguing, given that they are physically isolated from the digestive system of the host, through which the substrate passes.

(A)

(B)

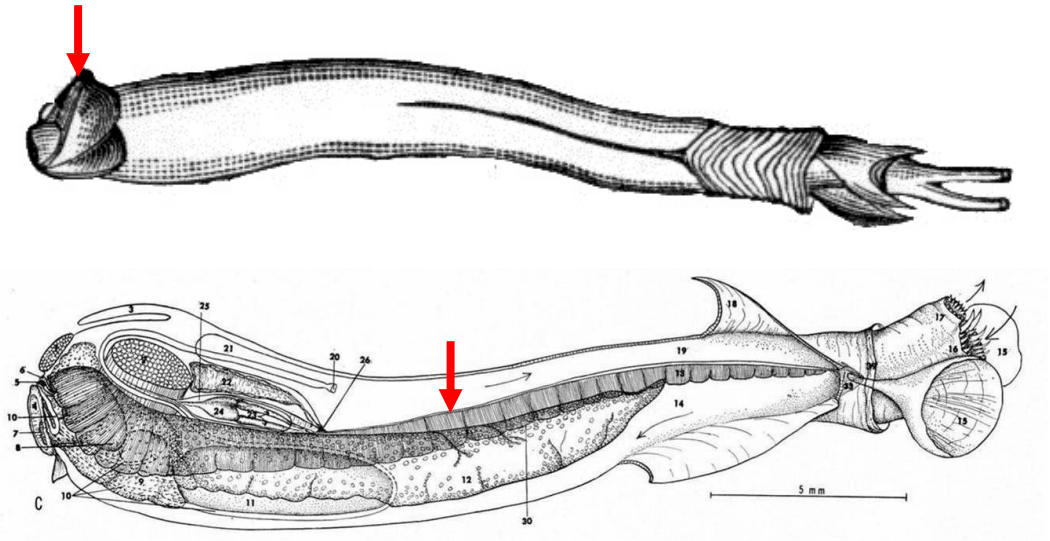

Figure 1.1 (A) Cartoon depiction of a typical shipworm, adapted from the directory of mollusks at Slippery Rock University (http://srufaculty.sru.edu). Arrow indicates the location of the reduced shell. (B) Anatomical sketch of *Teredora malleolus* showing the extended gill that harbors bacterial endosymbionts (red arrow), adapted from catalogue of the Teredinidae (Turner, 1966).

While the overall composition of wood is highly variable, heterogeneous, and often species- or genus-specific, the main components of woody plant cell walls include cellulose (40-45%), hemicellulose (25-40%), and lignin (20-30%) (Figure 1.2.A) (Lewin

& Goldstein, 1991). Each of these materials requires the specific activity of one or more enzymes to facilitate its enzymatic degradation. For the complete hydrolysis of cellulose, a suite of at least three enzyme classes is required: endo-1,4-*β*-glucanase (EC 3.2.1.4) to break *β*(1→4)-glucosidic linkages, exo-1,4-*β*-glucanase (EC 3.2.1.91) to remove either cellobiose or glucose from the non-reducing end, and 1,4-*β*-glucosidase (EC 3.2.1.21) to hydrolyze cellobiose or other cellodextrins to glucose (Figure 1.2.B) (Eriksson *et al.,* 1990).

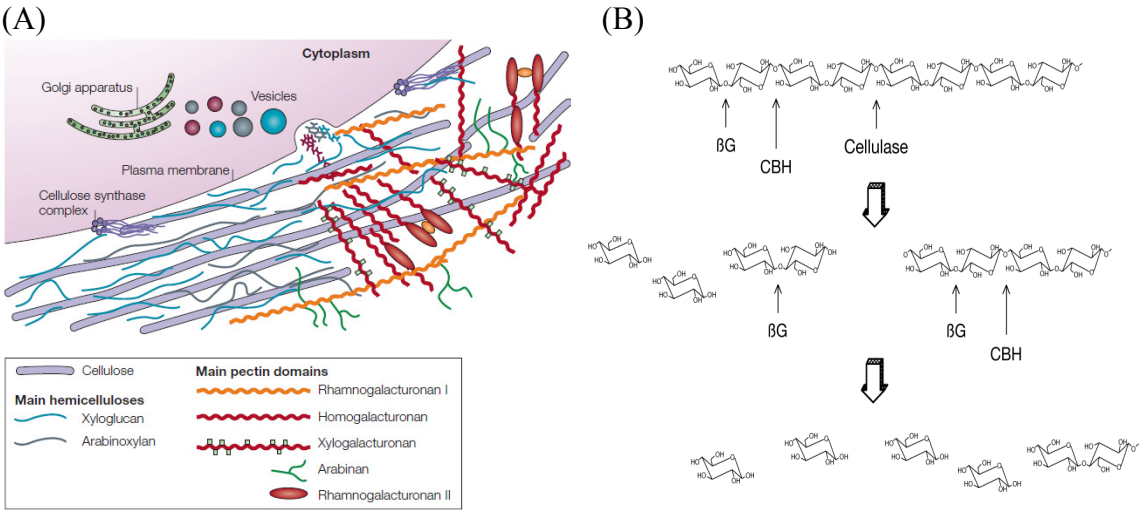

Figure 1.2 (A) Schematic representation of a typical plant primary cell wall showing cellulose microfibrils (purple rods) and a composite of matrix polysaccharides (from Cosgrove, 2005). (B) Mechanism of enzymatic hydrolysis of cellulose, showing the sites of attack on β-1,4 glucosidic linkages of cellulose by cellulase, cellobiohydrolase (CBH), and β-glucosidase (βG) indicated by arrows (from Clarke, 1996).

Genomic and laboratory data suggest that one of the shipworm symbionts, *Teredinibacter turnerae* strain T7901, possesses an extraordinary number of genes encoding enzymes active against complex polysaccharides (123 ORFs in total), which make this strain able to fully degrade cellulose and other components of complex polysaccharide mixtures autonomously (Yang *et al.,* 2009). This level of devotion to degradation of complex polysaccharides is comparable to that of *T. turnerae*'s closest known free-living relative, *Saccharophagus degradans* strain 2-40, containing about 130 ORFs encoding polysaccharide-active enzymes in its genome (Weiner *et al.,* 2008; Ekborg, 2005). Although the absolute number and classification of carbohydrate-active

enzymes is similar between *T. turnerae* T7901 and *S. degradans* 2-40 (Table 1.1), the proportion of these enzymes predicted to be specifically active against woody plant materials is far greater in the *T. turnerae* genome (Figure 1.3). The variety and specific activities of carbohydrate-active enzymes produced by *T. turnerae* T7901 make it of great interest for the development of cellulose-derived biofuel applications.

Table 1.1 Comparison of hypothetical carbohydrate-active proteins found in *T. turnerae* and *S. degradans* genomes, showing similar abundance of each enzyme family (adapted from Yang *et al.,* 2009).

	T. turnerae	*S. Degradans*
Glycoside Hydrolases	101	130
Polysaccharide Lyases	5	33
Carbohydrate Esterases	22	15
Carbohydrate Binding Modules	117	136

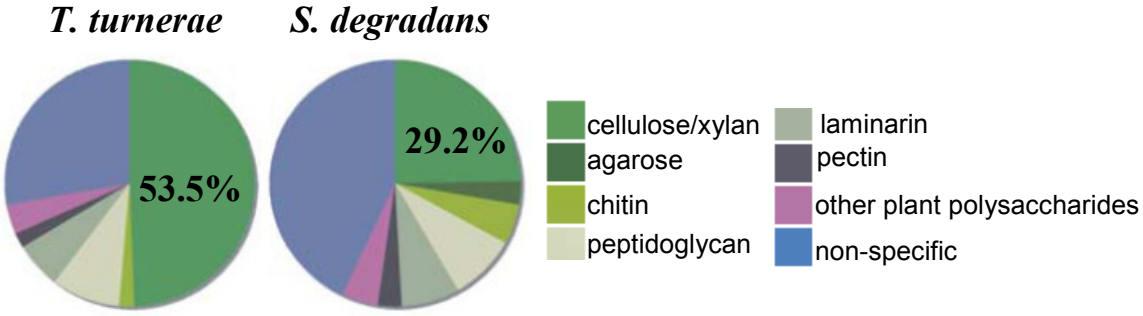

Figure 1.3 Fraction of glycoside hydrolase domains represented as a function of predicted substrate specificity shows that *T. turnerae* is highly specialized to degrade polysaccharides associated with terrestrial woody plant materials, including cellulose and xylan (adapted from Yang *et al.,* 2009).

Although wood proves to be an exceptional source of carbohydrate with the proper repertoire of polysaccharide-active enzymes, it contains only 0.03-0.1% nitrogen on a dry weight basis (Cowling & Merrill, 1966), requiring the shipworm and its symbionts to acquire nitrogen from an alternative source. The genome of *T. turnerae* contains a complete set of *nif* genes that enable it to fix atmospheric nitrogen (Yang *et al*., 2009), and its ability to do so has also been demonstrated experimentally (Distel *et al.,* 2002). Recently, it has been shown that nitrogen fixed by *Lyrodus pedicellatus* bacterial

symbionts, likely including *T. turnerae* strains, is transferred to the host so that it may use the symbiont-fixed nitrogen for its own biosyntheses (Lechene *et al*., 2007). The presumed role of *T. turnerae* in the shipworm symbiosis becomes quite clear when we consider its diazotrophic and cellulolytic capacities; two abilities rarely possessed by one aerobic bacterium.

In most well-characterized marine invertebrate-bacteria symbioses, such as the protobranch bivalve *Solemya velum* (Eisen *et al.,* 1992) and polychaete annelid *Riftia pachyptila* (Distel *et al.,* 1988) that harbor chemoautotrophic bacteria, or the bryozoan *Bugula neritina* that harbors a close relative of *T. turnerae,* "*Candidatus* Endobugula sertula" (Haygood & Davidson, 1997), a single bacterial symbiont is detected by 16S rRNA gene sequence analysis. Contrarily, multiple (up to four) genetically distinct bacterial symbionts have been observed within a single shipworm host (Distel *et al.,* 2002; Luyten *et al*., 2006), and *T. turnerae* is believed to comprise roughly 10% of the bacterial consortium present in the gill of *L. pedicellatus* (Luyten *et al*., 2006). To the benefit of the researcher, *T. turnerae* is cultivable in the lab, which has assisted in our detailed characterization of this symbiont. However, cultivation of many of the remaining ~90% of bacterial symbionts in *L. pedicellatus* has proven difficult, so inferring their role in the symbiosis is more challenging. While the present work only pertains to *T. turnerae*, we must keep in mind that it is indeed a minority within the endosymbiont community.

Another notable feature of *T. turnerae* strain T7901 is the proportion of its genome that is dedicated to secondary metabolite biosynthesis, a topic of utmost interest in the present work. Based on genetic analysis, 7.1% of all genes and 36% of genes involved in cellular processes are involved in secondary metabolite biosynthesis, constituting nine predicted gene clusters (Yang *et al*., 2009). This ratio of secondary metabolite genes is comparable to that observed in industrially-relevant filamentous actinomycetes that produce most of the bioactive metabolites currently applied in medicine and agriculture. *Streptomyces coelicolor* and *Streptomyces avermitilis*, for example, have 5% and 6.6% of their genomes dedicated to secondary metabolite biosynthesis, respectively (Donadio *et al.,* 2002; Ikeda *et al.,* 2003; Bentley *et al*., 2002). The sheer investment *T. turnerae* has in biosynthesis of secondary metabolites powerfully illustrates the potential for finding novel bioactive metabolites within its genetic potential,

which may have essential functions in the symbiosis and the promise of biotechnological applications.

A closer look at the composition of the secondary metabolite gene clusters further assures us that we will find complex and unusual metabolites. Regions 2, 5, and 9 are predicted to contain modular type I polyketide synthetase (PKS) genes, ranging from 8Kb to 48Kb (Figure 1.4) (Yang *et al.*, 2009). The modular nature of these catalytic domains suggests that their final product will be roughly proportional to the size of the gene cluster, so the product of region 2 (48Kb) is likely to be much larger and structurally complex than the product of region 9 (8Kb), for instance. Regions 4, 6, and 7 are predicted to encode non-ribosomal peptide synthases (NRPS), while regions 1, 3, and 8 contain both PKS and NRPS elements (Yang *et al*., 2009).

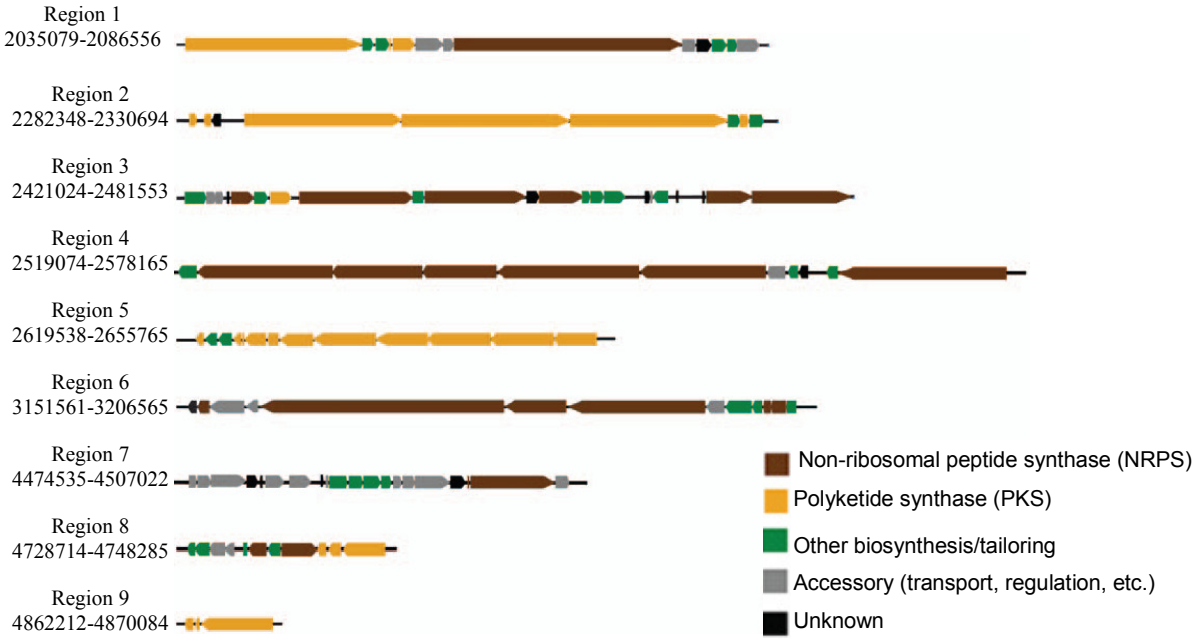

Figure 1.4 Nine predicted secondary metabolite gene clusters in the genome of *T. turnerae* T7901. Clusters are numbered in order of their distance from the origin of replication, and the coordinates are indicated beneath each region number (adapted from Yang *et al*., 2009).

Furthermore, some of these regions encode amino acids with significant sequence similarity to known producers of bioactive metabolites. For example, NRPS and PKS genes in regions 1 and 2 share about 50% amino acid sequence similarity with an NRPS and PKS of *Bacillus amyloliquefaciens*, which produces difficidin (Arguelles-Arias *et al*., 2009), bacillaene (Moldenhauer *et al*., 2010), and bacillomycin D (Koumoutsi *et al*.,

2004). That being said, the fact that half of the amino acid sequence encoded by these genes is heterologous and does not have significant BLAST hits to other genomes suggests that the gene products are novel and may have a different mode of biological activity.

Region 7 genes show homology to those required for the biosynthesis and transport of a catecholate siderophore (Yang *et al*., 2009), and phylogenetic analysis of the amino acid sequence encoded by the NRPS adenylation domain in this region suggests that it shares structural similarity to vanchrobactin, a siderophore produced by *Vibrio anguillarum* (Trindade-Silva *et al*., 2009). Chelation of Fe(III) by these low molecular weight, ferric-specific ligands (siderophores) with subsequent internalization by specific transporters and cell surface receptors is one of the strategies microbes have evolved for iron acquisition in response to this essential cofactor being poorly soluble in modern oceans, thus presenting a bioavailability issue (Anbar & Knoll, 2002). Other strategies of iron acquisition employed by microbes include utilization of ferritin or other protein-complexed iron, and reduction of extracellular Fe(III) to Fe(II) followed by transport of Fe(II). Although iron is a cofactor for many redox enzymes and plays a role in important biological processes such as respiration, N_2 fixation, methanogenesis, and DNA biosynthesis, intracellular iron concentration must be tightly regulated due to its ability to catalyze the generation of toxic free radicals.

Chapter 3 of this work includes a more detailed discussion of the regulation of the siderophore system in *T. turnerae* as well as data from differential expression analysis in iron-limited, phosphate-limited, and cellulosic media using microarrays. Chapter 4 discusses quantitative reverse transcription PCR analysis of three of the secondary metabolite gene clusters that showed the most dramatic differential expression pattern in the microarray analysis, to corroborate these findings. Chapter 5 includes mass spectrophotometric analysis of *T. turnerae* outer membrane proteins to identify receptors that are iron-regulated, and that may be utilized for ferric-siderophore uptake. Chapter 6 begins to characterize the biological activity of some of the secondary metabolites using bioassays, and identifies some organisms that show susceptibility to them.

Chapter 2

Aim of Research

Genomic and laboratory data have shown that *Teredinibacter turnerae* T7901 has an unusual combination of physiological traits that enable it to fix nitrogen, degrade cellulose, and produce bioactive secondary metabolites. This combination of abilities suggests that this symbiont has an essential role in the symbiosis by providing nutritional support to its host, and possibly chemical defense by secreting bioactive molecules that ward off predators and/or competitors. Prior studies of shipworm-symbiont symbioses have focused on the nutritional role of the symbiont(s), and have not thoroughly investigated the function of the repertoire of secondary metabolites produced by the symbiont, or their prospective applications.

Primarily, the current study sought to evaluate differential expression of *T. turnerae* T7901 secondary metabolite genes in response to specific nutrient limitations to better understand the regulatory schemes in place. Additionally, correlating upregulation patterns of secondary metabolite genes with positive bioassay results was used as a way to deduce which gene clusters may be responsible for the production of bioactive secondary metabolites. Because genomic data suggests that some of the secondary metabolites are extremely large and structurally complex, complete synthesis will be mechanistically difficult in the event that these molecules reach industrial production. These expression studies help optimize biosynthesis of secondary metabolites of interest for further characterization, structure elucidation, and eventual semi-synthesis or direct production for industrial applications.

Similarly, differential expression of genes involved in complex polysaccharide degradation was evaluated when grown on different carbon sources. Understanding the

regulation of these genes will facilitate maximal enzyme production for potential biofuel applications.

Chapter 3

T. turnerae Transcriptome Analysis by Microarray

3.1 Introduction

Gene regulation by iron availability

While iron is required by most bacteria (*Lactobacillae* [Archibald, 1983] and some spirochetes [Posey, 2000] are the only known exceptions) as a cofactor for many redox enzymes, its intracellular concentration must be exquisitely regulated due to its ability to catalyze the formation of free radicals in the presence of oxygen via Fenton's reaction (Winterbourn, 1995). Marine bacteria that require iron are likely faced with the constant challenge of scavenging it, due to modern oxic and neutral oceans facilitating the formation of poorly-soluble iron hydroxides. Siderophores are a common coping mechanism addressing this iron bioavailability issue, which allow microbes to chelate iron in the extracellular environment and then deliver it in a complexed form back to the cell for internalization by specific cell surface receptors. Strict regulation of expression of siderophore biosynthetic and receptor genes is a common method to maintain iron homeostasis, and this regulation is often imposed by the ferric uptake regulator (Fur) protein (Althaus *et al*., 1999; Escolar *et al*., 1999; Wee *et al*., 1988). In iron-replete conditions, Fur interacts with Fe^{2+} and undergoes a conformational change that allows it to bind to cognate DNA sequences ("Fur boxes"), and exert transcriptional repression on iron-regulated promoters. Utilization of Fur in regulation of siderophore systems is widespread, and homologues of the *fur* gene have been described in multiple phyla of domain Bacteria, including *B. subtilis* (Bsat *et al*., 1998) and *Vibrio cholerae* (Litwin *et al*., 1992), for example, as well as cyanobacteria. The genome of *T. turnerae* contains two

fur homologues (genes TERTU_0053 and TERTU_3389), and bioinformatic analysis suggests that there are two putative Fur boxes at intergenic spaces within the putative siderophore biosynthetic gene cluster, secondary metabolite region 7 (Trindade-Silva *et al*., 2009). Recently, several subclasses of Fur homologues have been identified, and were shown to be involved in processes not directly related to iron homeostasis, such as acid tolerance and protection against oxidative stress (Hernandez, 2004; Pohl *et al*., 2003). In spite of the number of putative Fur homologues conveniently matching the number of hypothetical Fur boxes in the *T. turnerae* genome, it is possible that one of the Fur proteins has an altogether different function, and that both Fur regulons are under the transcriptional regulation of the same Fur protein.

Siderophores are also of interest due to their potential as drug delivery agents. This "Trojan Horse" method of drug delivery exploits the specificity of cell surface receptors and uses the same entry route as the native siderophore to deliver a siderophore-drug conjugate to the organism of interest (Miller *et al*., 2009; Roosenberg *et al*., 2000). It has been demonstrated that siderophore analogues or foreign siderophores with sufficient structural similarity can utilize the native siderophore uptake system (Balado *et al*., 2009), so a *T. turnerae* siderophore-drug conjugate could be used to target the vanchrobactin-producing fish pathogen, *Vibrio anguillarum*, for example.

Because the *T. turnerae* genome contains homologues of all of the genes for a Fur-regulated iron acquisition system, a growth medium resulting in iron starvation of *T. turnerae* was developed in order to analyze the global changes in gene expression that resulted, using microarrays.

Gene regulation by inorganic phosphate availability

Historically, the majority of new drugs have been generated from natural products or their derivatives (Harvey, 2008), and with pathogenic microbes becoming resistant to current treatment options, the urgency for novel drug discovery is pressing. There are currently more than 100 compounds derived from natural products in clinical trials for use as antimicrobials, cancer treatment, and neuropharmacological therapeutics, among other applications.

Inorganic phosphate (P_i) has been repeatedly demonstrated to exert negative regulation of antibiotics and other secondary metabolites at the level of transcription in a broad spectrum of bacteria (Martin, 2004). Among the natural products regulated by P_i are candicidin, cephalosporin, cephamycin, neomycin, tetracycline, and dalbavancin, to name a few (Liras *et al*., 1990; Alduina *et al*., 2007). These P_i-regulated systems commonly employ a two-component regulatory system, such as the PhoR-PhoP system that regulates antibiotic biosynthesis in *S. lividans* and *S. coelicolor* (Sola-Landa *et al*., 2003; Anderson *et al*., 2001). In this system, PhoR is a membrane sensor kinase, and PhoP is a response regulator that binds cognate DNA sequences in promoter regions ("*pho* boxes"). In *E. coli* and *B. subtilis*, the PhoP protein becomes phosphorylated in response to P_i starvation, and acts as a transcription factor by binding to the *pho* box upstream of the phosphate-regulated genes (Martin, 2004). In P_i-replete conditions, however, there is often a transition between secondary and primary metabolism, because the *pho* regulon genes become silenced and enzymes in central primary metabolic pathways, such as phosphofructokinase and glucose-6-phosphate dehydrogenase, become stimulated. PhoR and PhoP homologs were detected in the genome of *T. turnerae* (TERTU_4562 and TERTU_4563, respectively) along with several other putative two-component regulatory systems, suggesting a similar phosphate regulatory system may be in place.

Due to the ubiquity of phosphate regulatory systems among major secondary metabolite producers, it was of interest to look at expression of all of the *T. turnerae* secondary metabolite genes in response to P_i starvation.

Differential expression of carbohydrate-active genes

As the primary constituent of lignocellulosic biomass, cellulose is the most abundant organic compound on earth, and its microbially-mediated degradation and conversion to ethanol shows promise as an eventual sustainable alternative to conventional oil-based fuels. One of the many obstacles to enzymatic degradation of cellulose within lignocellulosic material is physical obstruction of substrate imposed by lignin and other matrix polysaccharides. Current practices utilize a conglomeration of

enzymes to combat the heterogeneity of lignocellulose, and require a chemical and heat pretreatment of the feedstock to achieve size reduction and increase substrate accessibility prior to enzymatic hydrolysis of cellulose to 6-carbon sugars (Hahnhagerdal *et al*., 2006; Binder & Raines, 2010). This pretreatment requires significant input of energy and costly materials, decreasing the overall efficiency of the process. As we sequence more genomes of cellulolytic microorganisms and characterize more carbohydrate-active enzymes, we're becoming increasingly aware of novel enzyme systems with a broad spectrum of polysaccharide substrates. *T. turnerae* shows promise in contributing to biofuel development due to its high degree of specialization in degradation of woody plant materials, and that it contains multicatalytic enzymes with distinct catalytic activities against different substrates, a rare occurrence (Yang *et al*., 2009). Expression analysis of *T. turnerae* carbohydrate-active genes in cellulosic and sucrose-based media using a microarray will assist us in our understanding of what regulates the biosynthesis of these enzymes that have central roles in the symbiosis, as well as great promise for cellulose-derived biofuel development.

3.2 Materials and Methods

Bacterial strain and culture conditions

T. turnerae T7901 (ATCC # 39867) was initially isolated by John Waterbury of Woods Hole Oceanographic Institution from the shipworm *Bankia gouldi* collected from Beaufort, North Carolina in 1979. Propagated culture of the original isolate was generously provided for this work by Dr. Waterbury, and was grown in a modified version of shipworm basal medium (SBM) (pH 8.0; adjusted with sterile 1M NaOH after autoclaving) as described previously (Distel *et al*., 2002), containing 0.5% (w:v) sucrose or cellulose (Sigma-Aldrich S6790), 5mM ammonium chloride, 20mM HEPES, and artificial seawater (Kester *et al.*, 1967) instead of natural seawater. Inoculum was prepared by growing cells on solid SBM (1.5% agar, w:v) for three days at 30°C, and transferring a single colony to a liquid preculture. Precultures were grown overnight at 30°C, and then used to inoculate fresh medium at 0.1% final volume (e.g. 100µL

overnight preculture to 100mL fresh medium). Baffled flasks with a capacity 2-2.5 times the volume of culture grown in them were used for liquid cultures (e.g. 250mL flask for 100mL culture volume, or 100mL flask for 50mL culture), and all glassware was acid-rinsed prior to use to remove residual metals. EDTA-chelated ferric iron (Sigma E6760) was added as the sole iron source at an appropriate concentration to result in iron-limited or iron-replete media. Potassium phosphate monobasic (Fisher BP362) was added from a sterile 1M stock solution to prevent coprecipitation during autoclaving, and allow for easy adjustment of phosphate concentration when required. Liquid cultures were incubated at 30°C and shaken at 125 RPM in an orbital shaker. Bacterial growth was monitored either by extracellular protein quantitation using the method of Bradford (Bradford *et al*., 1976) or by optical density with a multi-detection microplate reader (Molecular Devices SpectraMax M2^{e}) at 600nm. *T. turnerae* extracellular protein concentration in liquid medium was previously shown to be proportional to total cellular protein, and thus a reliable metric of cell growth (Ahuja *et al*., 2004; Greene *et al*., 1989). The strain and culture method described here was used consistently throughout this work and applies whenever *T. turnerae* is referenced.

To determine an iron concentration that would result in iron starvation of *T. turnerae* while permitting the culture to reach substantial cell density, liquid media were prepared from serially-diluted Fe-EDTA stock solutions, and premature stationary phase relative to the iron-replete control was pursued (Figure 3.2). After an iron concentration was identified that led to starvation, single nutrient limitation was confirmed in this culture condition by repeating it in duplicate, and at stationary phase one flask was supplemented with iron to match the initial concentration of the iron-replete control while the other culture remained unsupplemented. These culture supernatants were assayed for the presence of siderophores by the chrome azurol sulfonate (CAS) assay, as previously described (Figure 3.1) (Schwyn & J Neilands, 1987).

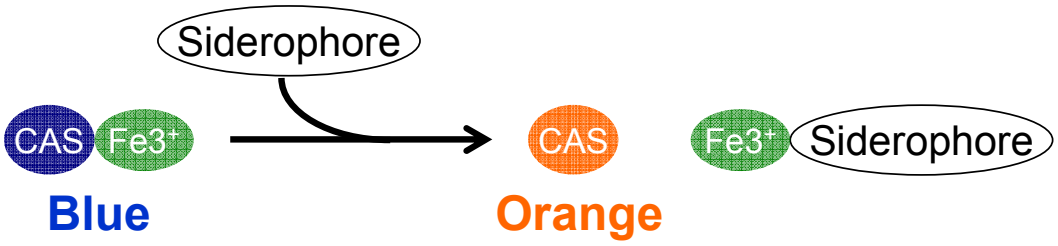

Figure 3.1 Principle of the single-displacement, colorimetric CAS reaction, which permits spectrophotometric quantitation of siderophores in culture supernatant.

Determination of phosphate limitation of *T. turnerae* liquid culture was carried out in the same manner as described above for iron limitation, with the exception of performing the CAS assay.

RNA Isolation and Preparation of Cy5-Labeled cDNA

Three separate microarray experiments were performed to evaluate differential gene expression of *T. turnerae* in iron-limited, phosphate-limited, or cellulosic media. The variable and reference group (control from which an expression baseline is generated) for each experiment is detailed in Table 3.1.

Table 3.1 Description of *T. turnerae* culture conditions used for microarray analysis. The variable condition is indicated in bold for each experiment. The incubation time indicates when cells were collected for RNA extraction from the designated culture.

Experiment	Description	Treatment Group	Iron (μM)	Phosphate (μM)	Carbon Source, 0.5% (w:v)	Incubation Time (hrs)
1	iron limitation	experimental	**0.113**	112.426	sucrose	36.5
		*reference	11.321	112.426	sucrose	36.5
2	phosphate limitation	experimental	11.321	**28.107**	sucrose	29
		reference	11.321	112.426	sucrose	29
3	cellulosic medium	experimental	11.321	112.426	**cellulose**	40
		*reference	11.321	112.426	sucrose	36.5

*The same culture was used as a reference group in iron limitation and cellulosic medium experiments.

For each experiment, 100mL *T. turnerae* modified SBM cultures were prepared in triplicate for experimental conditions, as well as for their reference culture condition. It should be noted that *T. turnerae* lag phase in cellulosic media is longer than that in a sucrose-based medium, so the cellulose experimental group was incubated longer than its sucrose reference group such that RNA was prepared from cells in a comparable

physiological state. A comparable cell density of these cultures was confirmed by extracellular protein quantitation.

Cells were pelleted by centrifugation (4000RPM, 20min, 4°C), and immediately lysed in 2mL TRIzol® reagent (Invitrogen 15596-018) per culture by repetitive pipetting. Total RNA extraction proceeded as per the manufacturer's protocol. Following a wash with 75% ethanol, the RNA was further purified by desalting and DNase digestion using an abbreviated protocol for the Illustra™ RNAspin mini RNA isolation kit (GE Healthcare 25-0500-70). Purified RNA was eluted in tris-EDTA buffer (pH 7.4; Fluka 93302) instead of water, to provide greater stability during downstream use, and electrophoresed with an Agilent 2100 Bioanalyzer to verify no degradation occurred during RNA extraction and/or storage at -80°C. The three RNA preparations were pooled from each culture condition to minimize the effects of growth and extraction variation. Pooled RNA was used as the template for reverse transcription using random hexameric primers (Invitrogen 48190-011) and SuperScript™ III reverse transcriptase (Invitrogen 18080-093). The RNA in the RNA/DNA duplex was cleaved with RNase H (Invitrogen 18021-014) for 20min at 37°C and unincorporated nucleotides were removed with a QIAquick Nucleotide Removal Kit (QIAGEN 28304). The resulting cDNA was labeled with Cy5 using a Label IT® μArray kit (Mirus Bio 8810), and unincorporated Cy5 was removed with Illustra ProbeQuant™ Micro Columns (GE Healthcare 28-9034-08). The cDNA and Cy5 concentration was determined with a NanoDrop ND-1000 (Thermo Scientific), and the labeled targets were dried with a Savant SpeedVac® Plus (Thermo Scientific SC110A) and stored in the dark at -20°C until use.

Microarray Hybridization and Data Acquisition

Custom 12K microarray chips (CombiMatrix) were designed in ProbeWeaver (version 1.0.10; CombiMatrix) against antisense targets of *T. turnerae* T7901 (GenBank accession number CP001614) using default design constraints and no background. Nine probes (three unique probes, in triplicate) were designed for each gene in the categories outlined in Table 3.2, and two unique probes were designed for all other genes in the genome, resulting in 12,000 probes in total.

Table 3.2 Gene categories with increased probe coverage on the custom 12K microarray chips used in these studies, and their corresponding hypothetical function. Genes in these categories had 3 unique probes in triplicate (9 probes total) designed to target the cDNA generated from their transcript, while all other genes in the *T. turnerae* genome had 2 unique probes.

Gene Category	Hypothetical Function
sec. met. regions 1-9	secondary metabolite biosynthesis and tailoring
Fur transcriptional regulators, iron transport	iron acquisition and transport, siderophore biosynthesis
glycoside hydrolase	hydrolysis of carbohydrate glycosidic bonds
polysaccharide lyase	cleavage of polysaccharide chains via a beta-elimination mechanism
carbohydrate esterase	catalysis of de-O or de-N-acetylation of substituted saccharides
other carbohydrate binding domain	carbohydrate-binding
type 6 secretion system	maintenance of symbiotic interaction, biofilm formation
type 2 secretion system	transport of carbohydrate active enzymes across inner membrane
nitrogen metabolism	nitrogen fixation & assimilation
quorum sensing	LuxR or GacS/GacA-mediated cell density-dependent gene regulation
MFP/RND transporter system	secretion of secondary metabolites
cation efflux pump transporter	increase tolerance of divalent metal ions
other ABC transporters	transport of various substrates across membrane
outer membrane secretion protein, type I	protein transport
sigma factors, sigma interacting proteins	transcriptional regulator
flagellar	chemotaxis and motility
two-component regulatory system / phosphate regulation/starvation	starvation sensor, response initiation
Fts family genes / various other housekeeping genes	for chip to chip and global normalization

Probe length ranged from 35-40 bases, with an average length of 35 bases. Calculated melting temperature of probes ranged from 70.00-75.00°C, with an average of 72.50°C. Probe uniqueness was tested by evaluating the strength of their cross-hybridization to the expected sequence space. The minimum margin between target melting temperature and closest secondary match was 17.75°C, which would essentially eliminate nonspecific hybridization.

Labeled cDNA groups were hybridized to microarray chips as recommended by the manufacturer. Hybridized and washed chips were scanned at 633nm with a ScanArray® 4000XL microarray analysis system (Perkin Elmer) at 5µm resolution, and the acquired images were saved as TIF files to be used in spotfinding software. These chips permit up to four sequential hybridizations per chip, with target removal in between each hybridization. Stripping of microarray chips was performed as recommended by CombiMatrix, and complete removal of targets was confirmed by scanning the chip in between hybridizations. When possible, duplicate hybridizations were performed with the reference group to ensure technical reproducibility.

Spotfinding was performed by manual template alignment in Microarray Imager (CombiMatrix). Signal intensities for treatment groups of each experiment were simultaneously quantile-normalized in ProbeWeaver (CombiMatrix), and background was calculated as the average of the foreground median of the lowest 5% of normalized

signal intensities. Spots displaying less than twice the background value were noted as possibly displaying insignificant expression. Signal intensities were transformed to $\log_2$ values to adjust for variance and allow for comparison between groups. Log_2 ratios were calculated by subtracting the $\log_2$ value of the reference group from that of the experimental group for a given spot in each experiment. Average $\log_2$ ratios were calculated for each gene.

3.3 Results and Discussion

Confirmation of iron or phosphate limitation in *T. turnerae* liquid cultures

To determine *T. turnerae* culture conditions that resulted in iron or phosphate starvation, the iron or phosphate concentration was incrementally decreased, and the growth kinetics were examined for evidence of limitation. Each order of magnitude decrease of iron concentration resulted in earlier stationary phase, and ultimately reduced cell density, as might be expected (Figure 3.2.A). Because *T. turnerae* can produce siderophores that chelate trace amounts of iron, it was able to grow even without the addition of any iron to the growth medium (Figure 3.2.A). On the other hand, *T. turnerae* lacks this type of specialized acquisition system for phosphate, an essential component of all living cells. This was reflected by a much lower tolerance for phosphate starvation, and cells began to lyse after 38hrs incubation in a medium without added phosphate (Figure 3.2.B). From these initial growth trials, iron and phosphate concentrations were selected that resulted in premature stationary phase relative to the iron or phosphate-replete control, yet allowed the culture to reach substantial cell density, as to generate sufficient RNA quantity for microarray analysis (calculated concentrations of 0.113μM Fe and 28.106μM PO_4 were selected). When these culture conditions were repeated in triplicate, supplementation of the iron- or phosphate-limited medium with the respective nutrient resulted in restoration of exponential growth and an ultimate cell density matching that of the control, suggesting that iron or phosphate was the only growth-limiting nutrient in each condition (Figure 3.2.C, D). Establishing these well-defined culture conditions that are deficient in a single nutrient allow us interpret expression data

and infer that any differential expression that is observed is directly or indirectly a response to iron or phosphate starvation.

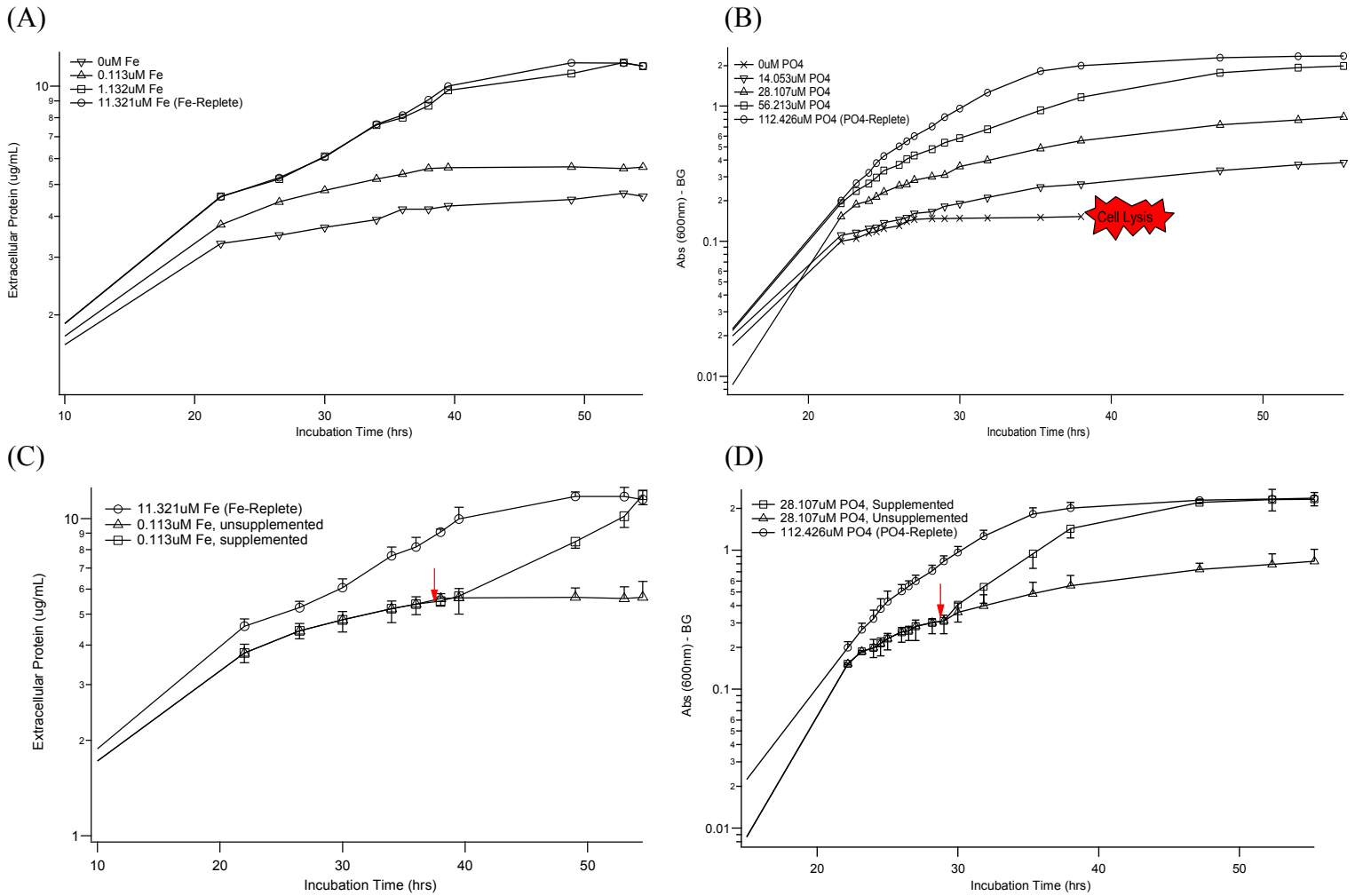

Figure 3.2 Growth curves of *T. turnerae* in liquid SBM with different (A) Fe and (B) PO_4 concentrations. Cells began to lyse after 38 hours growth in the absence of added PO_4 (0µM). (C) Fe and (D) PO_4 limitation were confirmed by starve-supplement growth trials performed in triplicate. Red arrows indicate when the culture was supplemented with Fe (37.5hrs) or PO_4 (28.5hrs), if at all, to match the initial concentration of the control, as well as when RNA was extracted for expression analysis.

Relative quantitation of siderophores in culture supernatants by CAS assay

Culture supernatants from the 37.5hr iron-replete and iron-limited SBM cultures were assayed for the presence of siderophores using the CAS assay (Figure 3.3). Uninoculated iron-replete SBM was used as a negative control because it contains a higher EDTA concentration than iron-limited SBM, which could result in false positive results for siderophore activity in this assay. However, this negative control did not show any difference in CAS activity relative to the inoculated iron-replete culture, likely because the EDTA in this medium is stoichiometrically matched to the iron concentration, leaving no unbound ligands available to participate in the CAS displacement reaction. This similarity in CAS activity between the negative control and iron-replete culture also provides evidence of iron sufficiency, because there is no effort invested in siderophore biosynthesis by the bacterium to acquire it. The iron-limited culture showed more than thirty two times the CAS activity than that of the iron-replete culture, suggesting far greater abundance of siderophores in this culture condition.

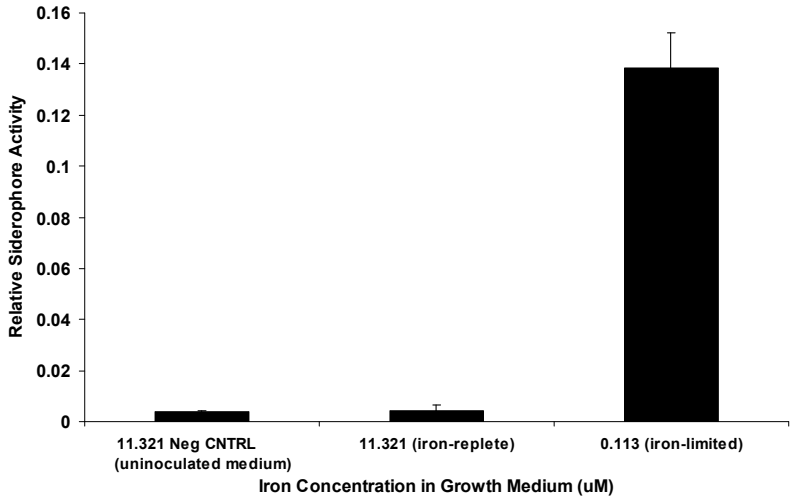

Figure 3.3 Relative siderophore activity of 37.5hr iron-replete and iron-limited *T. turnerae* SBM supernatants suggests greater abundance of siderophore in the iron-limited condition.

Assessment of RNA integrity

The *T. turnerae* RNA from triplicate cultures of each condition to be analyzed by microarray showed no evidence of degradation in the electropherograms generated from an Agilent Bioanalyzer (Figure 3.4). This RNA quality control step is essential to confirm that high integrity RNA is being used for analysis, because the mRNA is often subjected to rapid decay to meet dynamic cellular requirements, and microarray probes may not have sufficient sequence similarity to degraded targets to achieve hybridization. One way to assess bacterial RNA quality is to look at the ratio of 23S:16S rRNA in the sample. Although there is a 1:1 molecular ratio of 23S and 16S rRNA subunits in the bacterial ribosome, the 23S peak contains more nucleotides to bind the detection dye used in this electrophoresis method, and thus will integrate more area in the electropherogram. The 23S component is often more labile and prone to degradation, so a 23S:16S rRNA ratio greater than 1.5 generally suggests high quality RNA. A relatively flat baseline with minimal tailing to the left of the 16S and 23S rRNA peaks also would suggest that these subunits are intact, and the RNA sample is of high quality. All of the RNA samples for this analysis had a 23S:16S > 1.5, and showed minimal tailing of 16S and 23S peaks. For comparison, an electropherogram of an RNA preparation that failed the quality control (and was not used for downstream analysis), is shown (Figure 3.4.C).

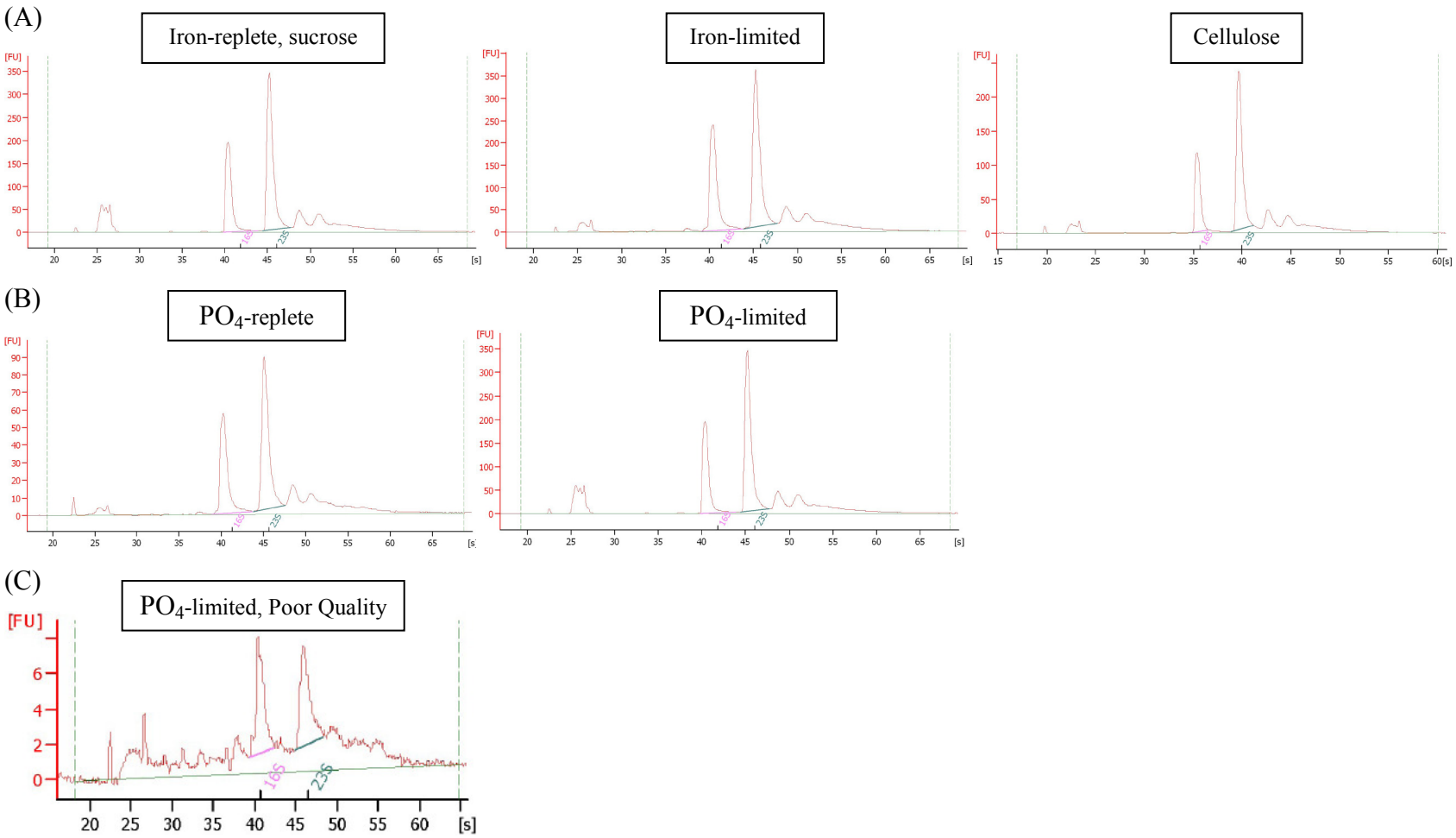

Figure 3.4 Representative electropherograms from each RNA treatment group used for expression analysis. Data was generated from an Agilent 2100 Bioanalyzer and is presented as fluorescence units [FU] as a function of runtime [s]. Labels above electropherograms describe the culture conditions from which the RNA was prepared, and positions of 16S and 23S rRNA peaks are indicated at the baseline. (A) Iron-replete, sucrose growth condition was used as a reference group in this expression analysis of the iron-limited and cellulose cultures, while (B) PO_4-replete growth condition was used as a reference for the PO_4-limited culture. (C) Electropherogram of poor quality RNA, included for comparison. This RNA sample was not used for expression analysis.

Differential expression of *T. turnerae* in response to iron starvation

The genome of *T. turnerae* contains two *fur* homologues, TERTU_0053 and TERTU_3389, and bioinformatic analysis suggests that there are two putative Fur boxes at intergenic spaces within secondary metabolite region 7 (Trindade-Silva *et al.*, 2009). This finding may suggest that this region is composed of two transcriptional units (TERTU_4055 to TERTU_4058, and TERTU_4059 to TERTU_4068), each of which may be regulated by a different Fur protein (Figure 3.5).

The second hypothetical Fur regulon contains homologues to genes of a *entCEBA*-like operon, which is required for the production and activation of 2,3-dihydroxybenzoic acid from the aromatic amino acid, chorismate. Also in this regulon is an *entF* homolog, encoding a non-ribosomal peptide synthetase, which is involved in the modular assembly of siderophore components in the case of enterobactin (Coderre & Earhart, 1989) and vanchrobactin (Balado *et al.,* 2006). Consistent with its annotation as a siderophore biosynthetic gene cluster, these microarray data show significant upregulation of region 7 in response to iron starvation, and the extent of upregulation of these genes also supports the notion of two transcriptional units within this cluster (Figure 3.5). The extent of upregulation of this region is also highly similar to that of the enterobactin producer *E. coli* (McHugh, 2003), and the vanchrobactin producer *Vibrio anguillarum* (Balado *et al*., 2008) in iron-limited growth conditions.

Downstream of the *entCEBA*-like operon, the second hypothetical Fur regulon encodes a membrane fusion protein (MFP; TERTU_4063) and resistance-nodulation-division (RND; TERTU_4064) protein, often part of a tripartite complex associated with active transport of various drugs and/or macrolides across the outer membrane (OM) (Figure 3.5) (Martin *et al*., 2009). Iron limitation resulted in a 1.9-fold increase in expression of TERTU_4063, and a 2.6-fold increase in TERTU_4064, suggesting that this MFP-RND operon may be involved in siderophore secretion (Figure 3.5).

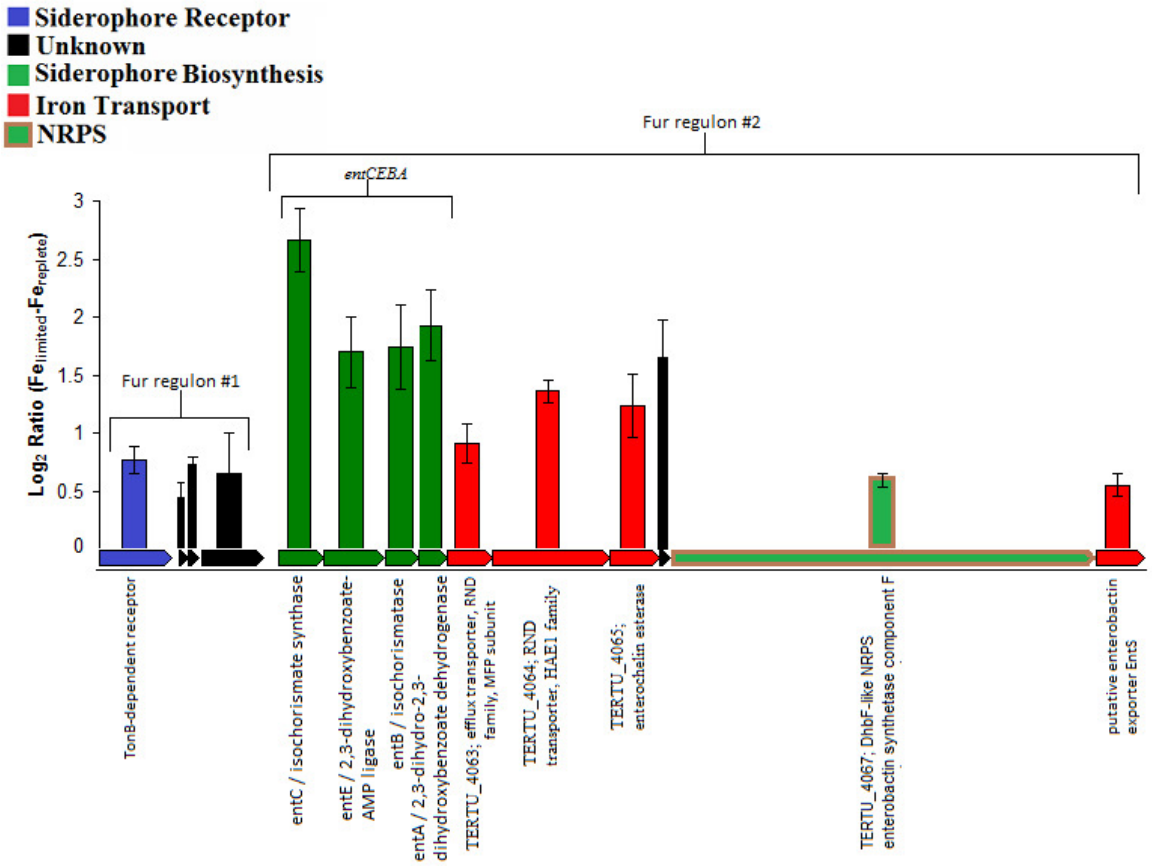

Figure 3.5 Relative expression of region 7 secondary metabolite genes show significant upregulation in response to iron starvation. Bars above each gene represent the $\log_2$ ratio of the iron-limited to iron-replete normalized signal intensities. The color of these bars corresponds to the hypothetical general function of the gene, if known, and the specific hypothetical gene product is indicated beneath the gene, if known. Error bars represent one standard deviation. Possible *entCEBA* components and Fur regulons, based on the position of hypothetical Fur boxes and the extent of upregulation, are indicated.

Uptake of ferric siderophores through the OM in Gram-negative bacteria is an active transport process, involving ligand-specific OM receptors. The energy required for the ferric siderophore to traverse the OM into the periplasmic space is derived from a cytoplasmic membrane-anchored protein complex, TonB-ExbB-ExbD, which transduces the energy of the proton motive force across the cytoplasmic membrane (CM) (Ahmer *et al*., 1995; Letoffe *et al*., 2004). Of the 33 identified TonB-dependent receptors in the *T. turnerae* genome, 13 of them were upregulated to varying degrees in iron-limited conditions (Figure 3.6.A). One of these TonB-dependent receptors (TERTU_2555) is

contiguous with a TonB protein (TERTU_2556), two ExbD homologs (TERTU_2557 & TERU_2558), and an ExbB homolog (TERTU_2559); all of which were upregulated in response to iron limitation, and together constitute a hypothetically-complete ferric-siderophore uptake system (Figure 3.6.B).

In *E. coli,* once the ferric-siderophore has been transported across the OM, a ferric-siderophore esterase is required for hydrolysis of the enterochelin moiety and subsequent release of ferrous iron into the cytoplasm (Langman *et al*., 1972). A homolog of this enterochelin esterase is present in the second hypothetical Fur regulon (TERTU_4065), and is also iron-regulated (Figure 3.5).

(A)

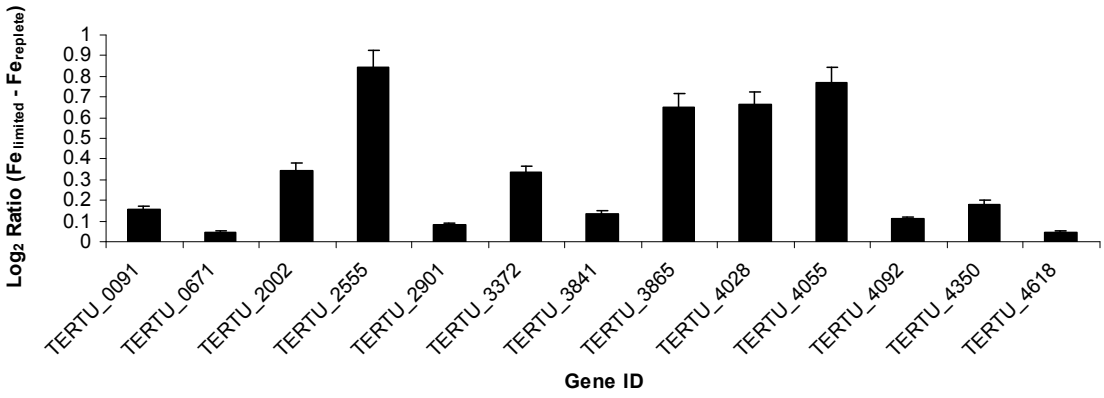

(B)

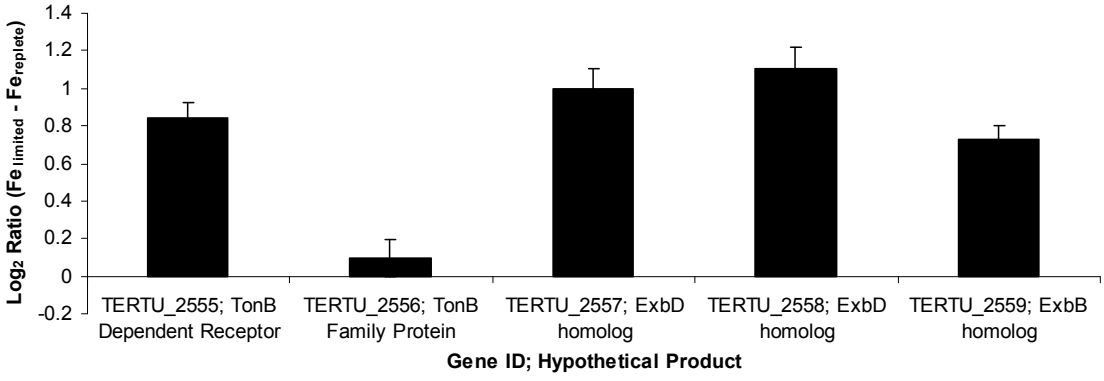

Figure 3.6 Relative expression of (A) hypothetical TonB-dependent receptors that were upregulated in iron-limited conditions and (B) a hypothetically-complete ferric-siderophore uptake system. The TonB protein (TERTU_2556) showed a lesser degree of upregulation than the other components, possibly because it interacts with other TonB-dependent receptors, and not only TERTU_2555.

Although genomic data indicates that *T. turnerae* produces a single siderophore, it's possible that it can utilize "foreign" siderophores produced by other microbes, or its own siderophore precursors that are still capable of iron chelation. Additionally, TonB-ExbB-ExbD complexes may transport substrates other than siderophores, such as vitamin B12 (Postle & Kadner, 2003) or host iron from heme (Wandersman & Stojiljkovic, 2000), which may explain why 13 TonB-dependent receptors are iron-regulated when it is presumably only producing a single siderophore.

These microarray data have identified iron-regulated elements in the genome that may be cooperatively responsible for the biosynthesis, secretion, uptake, and degradation/utilization of a catecholate-like siderophore. This study facilitates future genetic (mutant) studies by narrowing down the gene clusters responsible for these functions. Additionally, the description of the regulatory elements included here allows us to target overexpression of these genes for characterization of this siderophore and development of possible biotechnological applications.

Differential expression of *T. turnerae* secondary metabolite genes in response to phosphate starvation

This microarray analysis showed 213 genes to be upregulated at least 2-fold in P_i-limited conditions, 20 of which were secondary metabolite genes, and 11 of them in region 1. In fact, the expression of many secondary metabolite genes was altered upon P_i starvation, but most strikingly, region 1 was significantly and almost uniformly upregulated in this condition (Figure 3.7.A, B). Just outside of region 1 is a hypothetical two-component regulatory system, which may be the phosphate-sensing system that exerts regulation on region 1 expression. Region 2 also showed some evidence of upregulation in P_i-limited conditions (Figure 3.7.C).

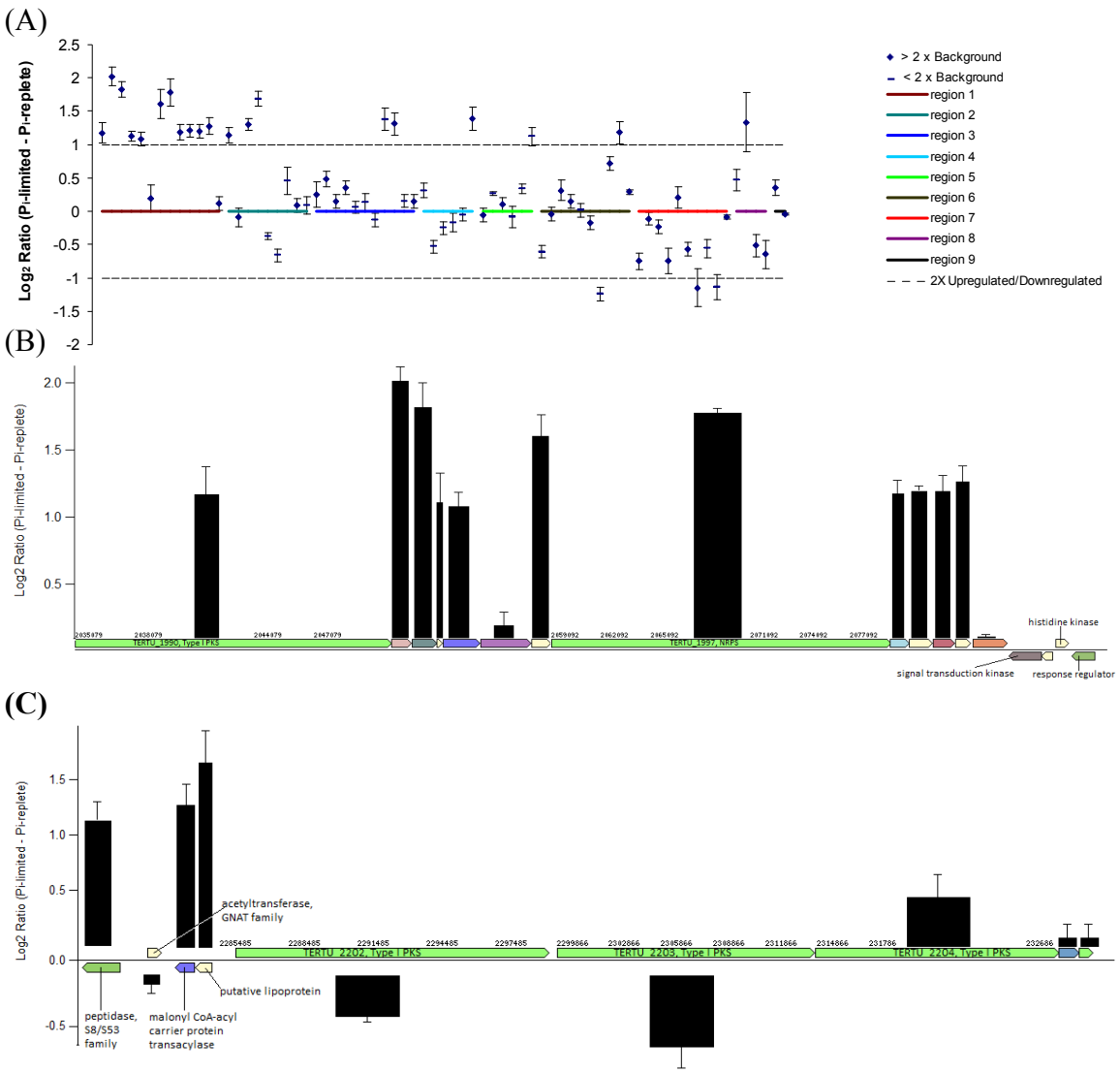

Figure 3.7 Relative expression of *T. turnerae* secondary metabolite genes in P_i-limited conditions. Data points represent the $\log_2$ ratio of the P_i-limited to P_i-replete normalized signal intensities. (A) All secondary metabolite genes show varying degrees of phosphate regulation; region 1 is most uniformly upregulated. Each point represents one gene, and the secondary metabolite region of a given gene is indicated by the color of the x axis. A diamond suggests the gene was expressed greater than 2 x background, whereas a dash indicates the gene was expressed less than 2 x background. (B) Region 1 secondary metabolite genes show strong regulation by phosphate. The positions of the PKS and NRPS, required for the biosynthesis of the final product of this cluster, are indicated. Just outside of this secondary metabolite region, a hypothetical two-component regulatory system is shown, which may be the phosphate-sensing system that exerts regulation on region 1 expression. (C) Some region 2 secondary metabolite genes are regulated by phosphate, although the PKS genes do not show a clear phosphate regulation pattern. Error bars represent one standard deviation.

Unexpectedly, several homologs of components of a type VI secretion system (T6SS) were found to be upregulated in P_i-limited conditions (Figure 3.8). Similar T6SSs have been shown to be a mechanism for communication between the host and symbiont, and an important virulence factor for some pathogenic bacteria such as *V. cholerae* (Bingle *et al*., 2008). This system may be capable of directly delivering effector proteins or toxins across both membranes of Gram-negative bacteria, as well as the host's plasma membrane (Filloux *et al.,* 2008). In this case, it is conceivable that it serves as an avenue for the symbiont to obtain phosphate from the host or as a lysis mechanism to escape the confinement of the bacteriocyte.

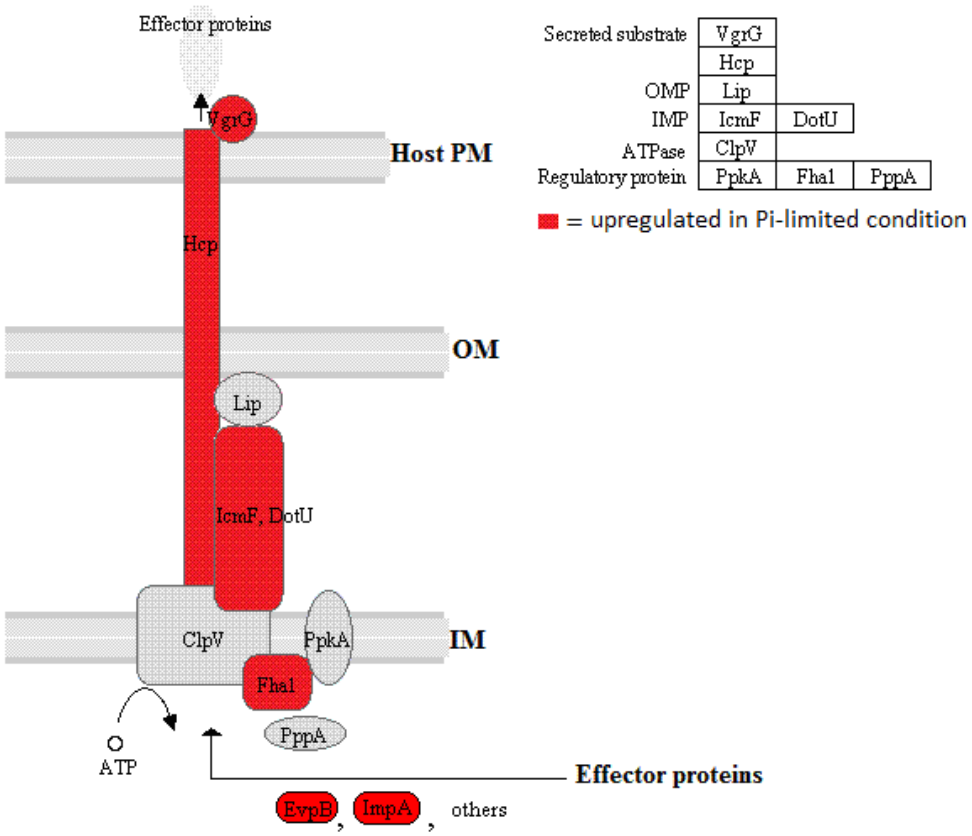

Figure 3.8 T6SS model showing a possible mechanism by which communication between symbiont and host is achieved by direct translocation of effector proteins across bacterial membranes, and into the host cell. Components of this hypothetical system that are significantly phosphate-regulated (≥2X upregulated in phosphate-limited conditions) are indicated in red. IM=inner membrane; OM=outer membrane; PM=plasma membrane.

Differential expression of *T. turnerae* carbohydrate-active genes in a cellulosic growth medium

Microarray expression analysis of *T. turnerae* carbohydrate-active genes showed that 58% of genes involved in polysaccharide degradation were highly expressed (≥3X background) in cellulosic and sucrose-based media, only 7% of which were differentially expressed at least two-fold (Figure 3.9).

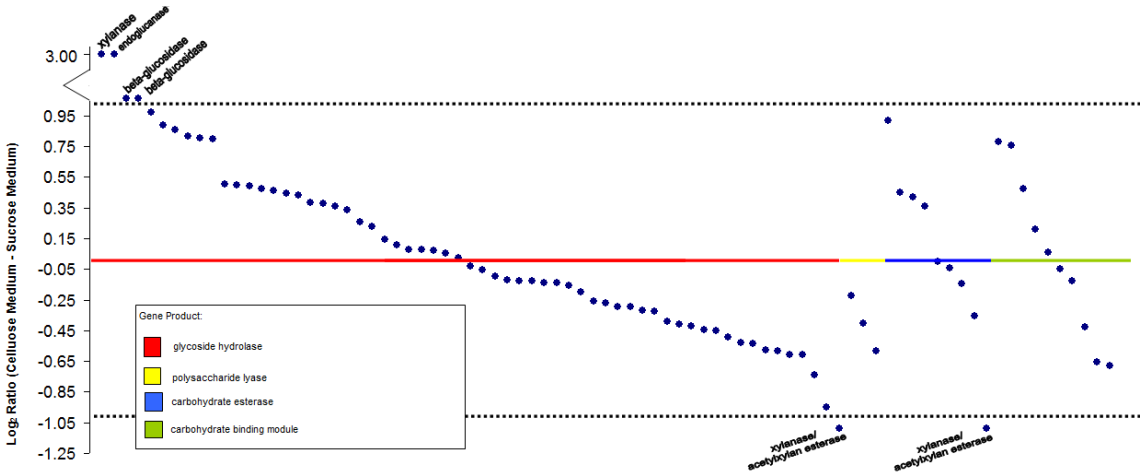

Figure 3.9 Relative expression of *T. turnerae* carbohydrate-active genes in a cellulosic medium. Data points represent the $\log_2$ ratio of the cellulosic medium to sucrose medium of normalized signal intensities. Each point represents one gene, and the class of the hypothetical gene product is indicated by the color of the x axis. If the gene was upregulated or downregulated more than 2-fold (dashed line), its specific activity is annotated.

Cellulose is an insoluble substrate and thus presents a detection issue for cells that degrade it. In most cellulolytic microbes, cellulolytic enzymes are produced constitutively at low levels, and then become upregulated in response to cellulose degradation products (e.g. cellobiose, cellobiono-l,5-lactone, or oxidized cellulose), and the final product of cellulose hydrolysis (glucose) results in repression (Tien & Kirk, 1988). Further confounding the regulation of cellulolytic enzymes in *T. turnerae* is its physical isolation from the digestive tract of the host, through which the substrate passes. I speculate that the insolubility and physical partition between cellulosic substrate and *T. turnerae* explains why there is little differential expression of carbohydrate-active genes

in cellulosic and sucrose-based media. Furthermore, being able to grow this organism on a sucrose-based medium, and maintain biosynthesis of cellulolytic enzymes, creates a fast and economical system for enzyme production. These results strengthen the candidacy of *T. turnerae* for the production of cellulolytic enzymes in biofuel applications.

Additional microarray data validation

In addition to the 12,000 custom probes, these microarrays included 544 factory-built controls, consisting of irrelevant probes (designed to target *Arabidopsis thaliana*, *Agrobacterium tumifaciens*, and phage lambda) and no-probe negative controls. The signal intensities obtained from these spots were ≤ background (data not shown), indicating minimal non-specific hybridization occurred on these microarrays.

The iron-replete, sucrose reference group was hybridized in duplicate to the same chip to assess the technical reproducibility in these analyses. 99.7% of $\log_2$ values from this duplicate hybridization showed less than a two-fold difference, suggestive of good technical reproducibility (Figure 3.10.A). Additionally, the expression levels of several "housekeeping genes" showed little variation between cellulose, iron-limited, and iron-replete sucrose media (Figure 3.10.B). Duplicate hybridizations of the P_i-replete reference group was not possible because the target stripping efficiency declined after the first two hybridizations, possibly due to minor dehydration of the hybridized chip, so the chip was discarded. Expression values of the P_i-limited group were not included in the housekeeping gene expression profile because phosphate starvation would likely lead to global changes affecting central cellular functions.

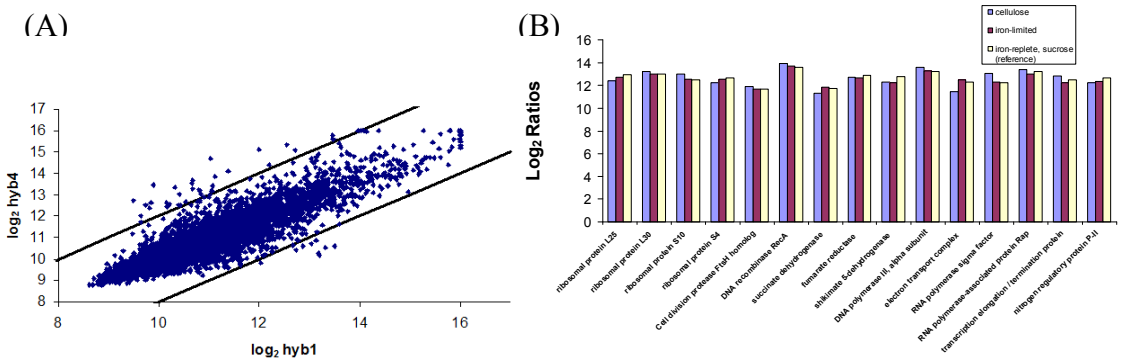

Figure 3.10 (A) 99.7% of $\log_2$ values from duplicate hybridization of the iron-replete, sucrose reference showed less than a two-fold difference, suggestive of good technical reproducibility. (B) Expression levels of "housekeeping genes" showed little variation between cellulose, iron-limited, and iron-replete sucrose media.

Chapter 4

Expression Analysis of Select Secondary Metabolite Genes by Quantitative Reverse Transcription PCR

4.1 Introduction

Although microarray expression analysis is a very powerful tool to observe global expression changes of treatment groups, quantitative reverse transcription PCR (qRT-PCR) allows us to analyze specific genes of interest with even greater acuity and accuracy. This method was chosen as a supportive analysis to the microarray findings by targeting genes required for the biosynthesis of a given secondary metabolite cluster.

In region 7, the putative TonB-dependent siderophore receptor and NRPS genes, partially responsible for the uptake and biosynthesis of siderophores, respectively, were selected for qRT-PCR analysis in iron-limited conditions. Because regions 1 and 2 showed the greatest extent of differential expression by microarray analysis in response to phosphate starvation, they were also targeted in this analysis. The PKS and NRPS genes, required for the biosynthesis of the final product, were selected for analysis of region 1, and the malonyl CoA-acyl carrier protein (ACP)-transacylase and acetyltransferase (AT) genes were targeted in region 2. The malonyl CoA-ACP-transacylase assists in the selection of an appropriate starter group (Crawford *et al*., 2006; Verbree, 1995), likely malonyl-CoA in this case, and the AT catalyzes the transfer of this starter group to the ACP domain (Shen, 2003). Together, the ACP-transacylase and AT comprise a starter unit, initiating the biosynthesis and elongation of the growing polyketide chain. TERTU_3044 (FtsZ, cell division protein) was included in these analyses as a housekeeping gene for reference.

4.2 Materials and Methods

Primers were designed using the National Center for Biotechnology Information (NCBI) primer design tool, Primer-BLAST, to amplify approximately 100bp of the middle of the gene of interest (Table 4.1). A minimum of one bp 3' GC clamp was included in each primer sequence to promote specific binding at the 3' end due to the stronger bonding of G and C bases. The center portion of the gene was targeted to mitigate any exoribonuclease degradation of the mRNA that may have occurred, and to detect transcripts that were terminated prematurely (Figure 4.1).

Table 4.1 Description of primers and their respective amplicon used for quantitative reverse transcription PCR analysis of *T. turnerae* secondary metabolite genes.

Gene ID	Secondary Metabolite Gene Region	Hypothetical Gene Product	Primer Sequence (5'→3')	Amplicon Genomic Position (From)	Amplicon Genomic Position (To)	Amplicon Size (bp)
TERTU_3044	N/A	cell division protein FtsZ	ACAGTCGCGTCGTGAGAGGC TACAGGGTGCGCGCGGTATC	3400340	3400435	115
TERTU_1990	1	modular polyketide synthase, type I	GCCAACGCAGCAGGTTGCAG TTGCGGTGTGGAAGGTGCCG	2039695	2039775	100
TERTU_1997	1	nonribosomal peptide synthetase	TATTGCCGACGGGCGAAGCG CCGCCGGACCATAGGCGTTC	2076046	2076122	96
TERTU_2198	2	acetyltransferase, GNAT family	TGTGGCTGGTGAAGAAGAGTCACTG CGCGGTCTAGATCGATGGGCG	2282528	2282626	119
TERTU_2199	2	malonyl CoA-acyl carrier protein transacylase	AGGCCGAGCACGGCGAAC GTCGCGCTTTTCGCAGCAGG	2284007	2284103	116
TERTU_4055	7	TonB-dependent receptor	ACTGACCGACAGCATCGCGG GAAGCAACTGCCGCCGCAAC	4484630	4484722	112
TERTU_4067	7	DhbF-like NRPS enterobactin synthetase	GGTGTGCGGCACGCGTAAAC AGTGCCACGGCGACGTTCTG	4500001	4500095	114

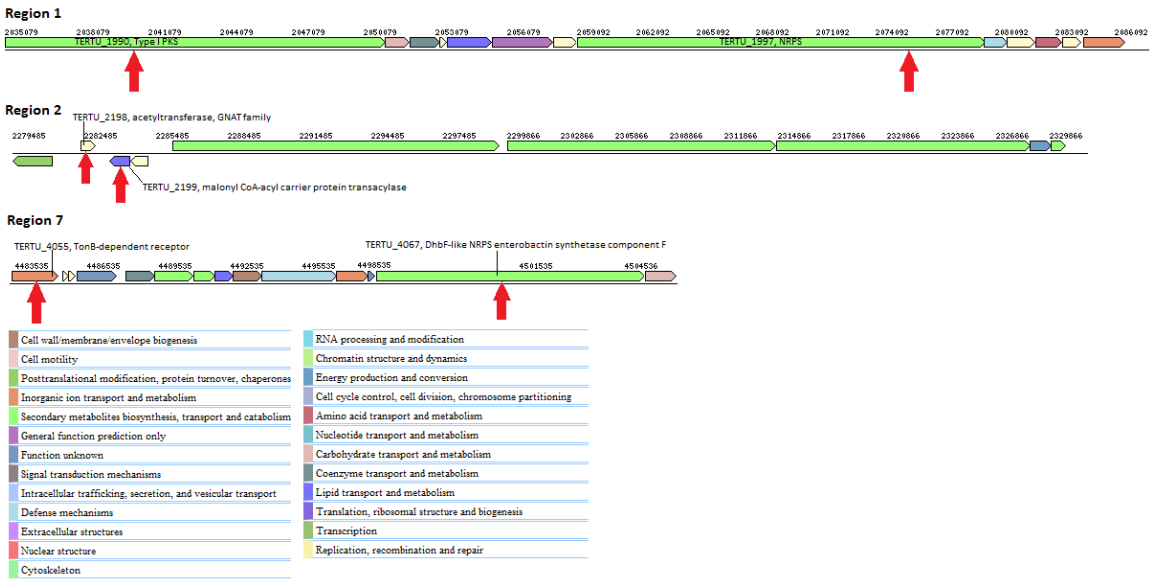

Figure 4.1 Genomic positions of *T. turnerae* secondary metabolite gene clusters 1, 2, and 7 that were targeted for qRT-PCR. Red arrows indicate the specific region of a gene from which approximately 100bp was amplified in this analysis. Gene IDs and hypothetical gene products are also provided.

Gradient PCR was performed on a BioRad iCycler™ Thermal Cycler to optimize the annealing temperature for each primer set. The amplicon from the PCR reaction that yielded a single, discrete band was purified with a QIAquick® PCR Purification Kit (QIAGEN 28106), cloned into a pCR®4-TOPO® plasmid (Invitrogen), and transformed into One Shot® TOP10 chemically-competent *E. coli* cells using a TOPO TA Cloning® Kit (Invitrogen K4575-02). Transformants were grown overnight at 37°C on LB plates with 50µL/mL ampicillin, and three colonies were transferred to glass test tubes with 5mL of liquid LB containing 50µL/mL ampicillin and grown overnight at 37°C at 200RPM. Plasmids from each clone were purified using a Plasmid Mini Kit (QIAGEN 12125) and sequenced using M13F (-20) (5'-GTAAAACGACGGCCAG-3') and M13R (5'-CAGGAAACAGCTATGAC-3') primers to confirm a single, and intended, genomic region of *T. turnerae* was introduced to each plasmid. Purified plasmids were quantified using a NanoDrop ND-1000 (Thermo Scientific) and stored at -20°C until they were used for the construction of a standard curve for qRT-PCR analysis.

A two-tube qRT-PCR protocol was used, and the cDNA was prepared by the same method described in section 3.2 for microarray analysis (up to the fluorescent labeling step) from RNA prepared at the incubation times indicated in Table 3.1. The unlabeled cDNA concentration was measured with a NanoDrop ND-1000 (Thermo Scientific) and stored at -20°C until use.

The qPCR portion of this analysis was performed in triplicate for each standard, no template control, and unknown reaction using a SYBR® Green qPCR SuperMix (Invitrogen 11733-038). Reaction volumes were 25µL and contained 500nM ROX reference dye, 200nM of the appropriate forward and reverse primer, and 100ng of total cDNA in the experimental reactions. qPCR reactions were carried out for forty cycles in a 96-well plate format on a StepOnePlus™ Real-Time PCR System (Applied Biosystems).

Threshold cycles (C_T) were calculated using the quantity of target, normalized to an endogenous control and relative to a reference sample using the $2^{-\Delta\Delta C_T}$ method (Livak 2001).

DNA Sequencing

All nucleic acid sequencing for this work was performed at the Oregon Health & Science University's West Campus Molecular and Cell Biology Core facility using an ABI 3700xL 96-capillary genetic analyzer (Applied Biosystems).

4.3 Results and Discussion

Supportive expression analysis of select secondary metabolite genes by quantitative reverse transcription PCR

The expression profiles from these qRT-PCR analyses (Figure 4.2) are remarkably similar to those seen in the microarray analysis (Chapter 3), providing additional assurance that the regulatory patterns observed are veritable. Once again, we see the TonB-dependent receptor and NRPS of region 7 are upregulated in iron-limited conditions, and the PKS and NRPS in region 1 are highly upregulated in P_i-limited conditions. The malonyl CoA-ACP-transacylase of region 2 did appear to be upregulated in P_i-limited conditions, although the AT did not show significant differential expression, suggesting that this cluster is not actively manufacturing its gene product. Being that these analyses show that only part of the starter unit was upregulated in P_i-limited conditions (the malonyl CoA-ACP-transacylase; TERTU_2199), it's conceivable that this gene cluster was in the preliminary stages of initiating transcription, and perhaps a different expression pattern may have been observed had the RNA been prepared slightly later in the growth phase. There was slight downregulation of FtsZ upon phosphate limitation, however, in retrospect this may be expected because nucleotide biosynthesis and cell division require phosphate and may be repressed in this condition.

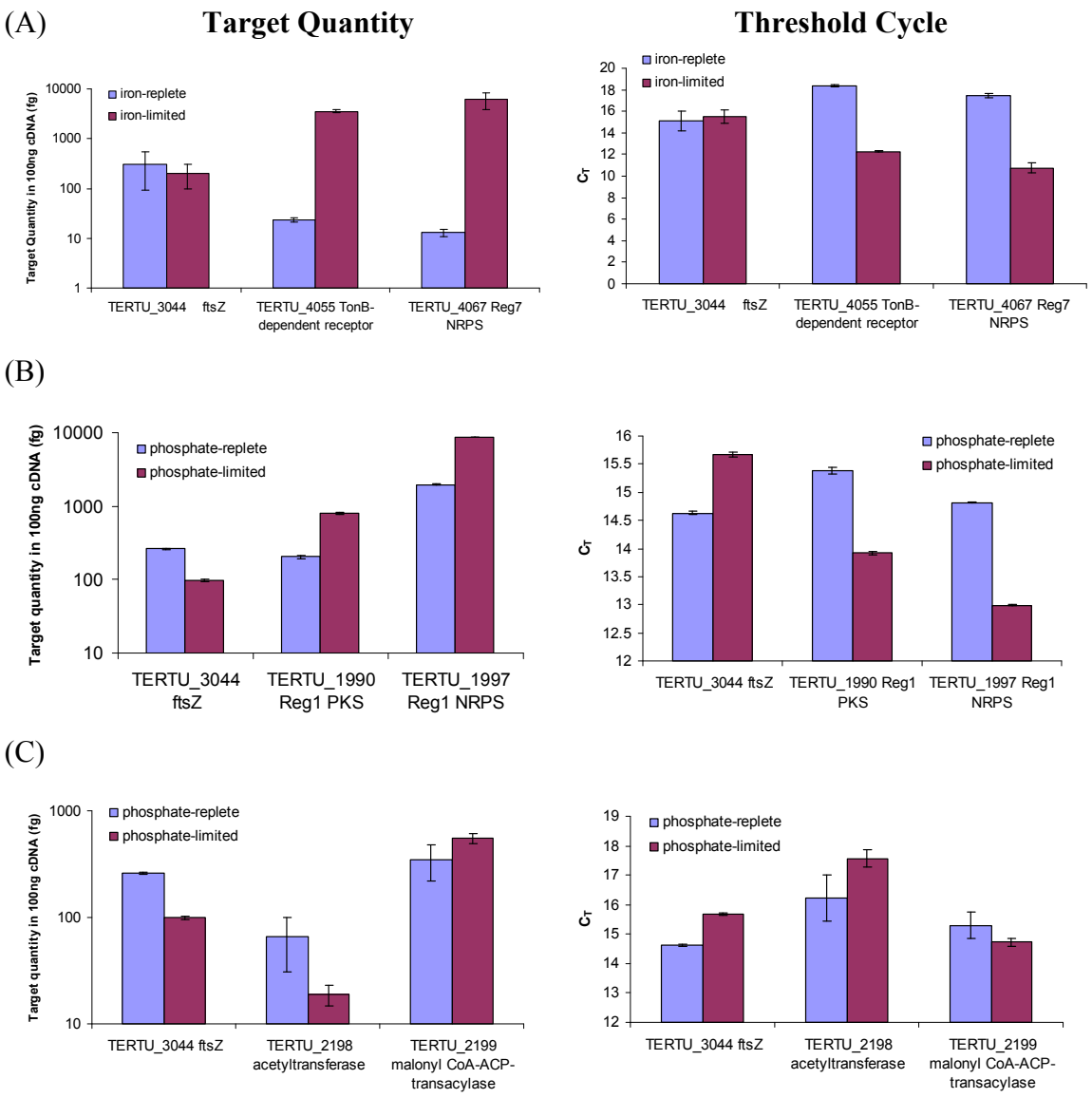

Figure 4.2 qRT-PCR expression analysis of select secondary metabolite genes. Target quantity is shown in the left column and C_T in the right. TERTU_3044 (FtsZ, cell division protein) was included in these analyses as a housekeeping gene for reference. Error bars indicate 1 standard deviation. (A) Region 7 TonB-dependent receptor, possibly involved in ferric-siderophore uptake, and NRPS, required for the biosynthesis of a catecholate-like siderophore. (B) Region 1 PKS and NRPS, required for the biosynthesis of the secondary metabolite product of this region. (C) Region 2 acetyltransferase and malonyl CoA-acyl carrier protein transacylase, comprising the starter unit of this gene cluster, and required for the initiation of biosynthesis and elongation of the polyketide chain.

Chapter 5

Isolation, Identification, and Relative Quantitation of *T. turnerae* Outer Membrane Proteins

5.1 Introduction

Although microarray (Chapter 3) and qRT-PCR (Chapter 4) expression analysis jointly provide convincing evidence that iron availability regulates the siderophore-mediated iron acquisition system in *T. turnerae*, we have yet to identify/quantify the proteins that actually carry out this process. In other words, demonstrating transcriptional regulation is circumstantial, but protein analysis provides direct evidence of a mechanism or process is underway, such as ferric-siderophore uptake. SDS-PAGE and LC-MS/MS analyses of outer membrane (OM) proteins were used as another approach to identify which TonB-dependent receptors are iron-regulated and may be utilized for ferric-siderophore uptake.

5.2 Materials and Methods

Isolation of *T. turnerae* outer membrane proteins

OM proteins were isolated at 37hr incubation from 100mL iron-replete and iron-limited *T. turnerae* SBM liquid cultures, essentially as described by Toranzo *et al*. (1983) and Crosa & Hodges (1981), with minor modifications. Briefly, after harvesting the cells by centrifugation (4000RPM, 20min, 4°C), they were resuspended in 10mL lysis buffer, consisting of 10mM Tris-HCl-0.3% NaCl (pH 8.0), and sonically treated with ten 30 second pulses at 20% amplitude (Branson Digital Sonifier® 250). After a 60 second

centrifugation (13,000 RPM in a tabletop centrifuge), the supernatant was decanted into a fresh tube, and the cell envelopes were harvested by another centrifugation for 1hr at 20,000 x *g* at 4°C. The cell envelopes were treated with 1.5% Sarkosyl in 10mM Tris-HCl for 20min at room temperature to dissolve the inner membrane. Outer membranes were collected by centrifugation for 1hr at 20,000 x *g* at 4°C, and retreated with 1.5% Sarkosyl to remove as much inner membrane material as possible. After another centrifugation for 1hr at 20,000 x *g* at 4°C, the outer membranes were washed three times with sterile distilled water, and stored at -20°C until use.

SDS-PAGE analysis of *T. turnerae* outer membrane proteins

Outer membranes were dissolved in 50µL of loading buffer, consisting of 62.5mM Tris-HCl (pH 6.8), 2% SDS, 10% glycerol, and 5% β-mercaptoethanol. Protein was quantified with a NanoDrop ND-1000 (Thermo Scientific) and adjusted with loading buffer to result in the same concentration for each sample. Bromophenol blue (0.001%) was added to the samples as a tracking dye, and 20µL of each OM prep was run through a precast 4-15% linear gradient polyacrylamide gel (BioRad 161-1392). The gel was washed three times for 5min with ultrapure water, and stained with an Imerpial™ Protein Stain (Pierce 24615) for 1hr with gentle agitation on a shaker. Excess stain was removed, and the gel was destained overnight in ultrapure water.

Identification and relative quantitation of *T. turnerae* outer membrane proteins by mass spectrometry

The gel was transferred to a glass Petri dish, and bands of interest were excised with a scalpel and washed with three changes of ultrapure water. To prepare the excised bands for an in-gel trypsin digestion, they were washed twice with 500µL of 100mM ammonium bicarbonate/acetonitrile (1:1), and dehydrated using a SpeedVac®. Dehydrated samples were reduced with 100µL of 10mM dithiothreitol (DTT) for 45min at 56ºC, then 100µL of 55mM iodoacetamide (IAA) for 30min at room temperature with gentle shaking. Excess DTT and IAA were removed and samples were washed with

500µL of 100mM ammonium bicarbonate/acetonitrile (1:1) for 15min at room temperature and dehydrated with a SpeedVac®.

Pretreated samples were digested with 100µL of trypsin digestion solution (10ng/µL trypsin in 100mM ammonium bicarbonate/acetonitrile [1:1]) for 15 min at 4ºC. 100µL of 100mM ammonium bicarbonate was added to the samples, and they were incubated overnight at 37 ºC.

The trypsin digest solution was transferred to a fresh tube and saved, and gel samples were washed with 50µL of 25mM ammonium bicarbonate for 15min at 37ºC. 50µL of 50% acetonitrile was added to the gels and incubated with shaking for 15min at 37ºC. This solution was removed and combined with the solution from the overnight digestion. 50µL of 5% formic acid was then added to the gel and incubated for 15min at 37ºC with shaking. 50µL of 50% acetonitrile was added, shaken for 15min at 37ºC, and the supernatant was pooled with the digestion and wash solutions. The combined supernatants were filtered through a 0.45µM filter, and concentrated to 10µL on a SpeedVac®.

Each protein digest was then analyzed by LC-MS using an Agilent 1100 series capillary LC system (Agilent Technolgies) and an LTQ Velos mass spectrometer (Thermo Fisher). Electrospray ionization was performed with an ion max source fitted with a 34 gauge metal needle (Thermo Fisher 97144-20040) and 2.7 kV source voltage. Samples were applied at 20µL/min to a trap cartridge (Michrom BioResources), and then switched onto a 0.5 x 250 mm Zorbax SB-C18 column with 5µM particles (Agilent Technologies) using a mobile phase containing 0.1% formic acid, 7-30% acetonitrile gradient over 95 min, and 10µL/min flow rate. Data-dependent collection of MS/MS spectra used the dynamic exclusion feature of the instrument's control software (repeat count equal to 1, exclusion list size of 100, exclusion duration of 30sec, and exclusion mass width of -1 to +4) to obtain MS/MS spectra of the three most abundant parent ions following each survey scan from m/z 350-2000. The tune file was configured without averaging of microscans, a maximum inject time of 10msec, and AGC targets of 1 x 105 in MS mode. Peptides were identified by comparing the observed MS/MS spectra to theoretical MS/MS spectra of peptides generated from a protein database using Sequest (Version 27, rev. 12, Thermo Fisher). DTA files were created with Discoverer 1.0

(Thermo Fisher), and Sequest searches configured with parent ion and fragment ion mass tolerances of 2.0 Da (average) and 1.0 Da (monoiostopic), respectively. The search was also performed using a static modification of +57 on cysteines due to alkylation with IAA, a differential modification of +16 on methionine, and trypsin specificity. Searches were preformed against a database containing *T. turnerae* sequences from version 40.12 of the swissprot + trembl database and common contaminant proteins. Reversed protein sequences were appended to the end of the database to provide quality control. Lists of identified proteins were assembled using the program Scaffold (version 2_06_00, Proteome Software). Thresholds for peptide and protein probabilities were set in Scaffold at 95% and 99%, respectively, as specified using the Peptide Prophet algorithm (Keller *et al*., 2002) and the Protein Prophet algorithm (Nesvizhskii *et al*., 2003), respectively, with a minimum of 2 peptides matched to each protein entry.

The trypsin digestion and MS analysis of these samples was performed at the Oregon Health & Science University Proteomics Shared Resource, which also provided technical advice and assistance with data interpretation.

5.3 Results and Discussion

Electrophoresis and LC-MS/MS analysis of *T. turnerae* outer membrane proteins

OM proteins from iron-replete and iron-limited cultures were separated by SDS-PAGE, and bands were excised from the gel in the size range where TonB-dependent receptors were expected based on their predicted size (55-130 kDa) (Yang, *et al.*, 2009), and showed increased band intensity in the iron-limited condition (Figure 5.1).

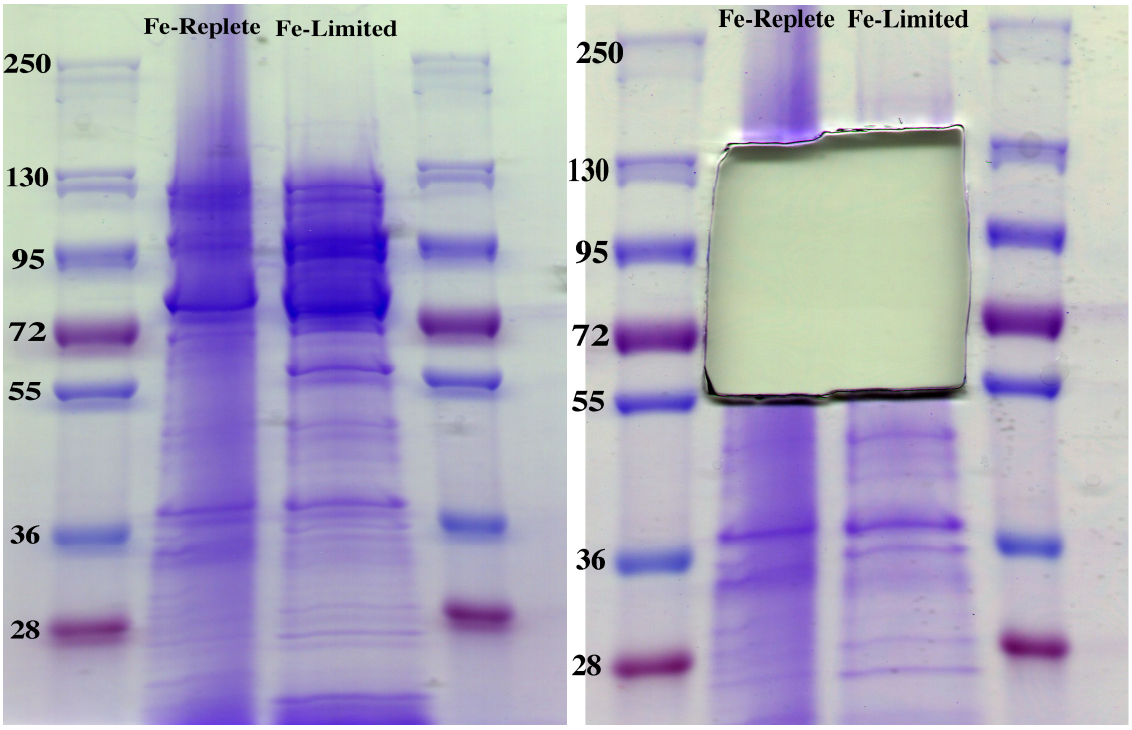

Figure 5.1 Linear gradient (4-15%) polyacrylamide gel of OM proteins isolated from iron-replete and iron-limited cultures. Image on right shows the same gel pictured on the left after bands were excised for LC-MS/MS analysis.

LC-MS/MS analysis of these bands identified about 400 proteins in total, some of which may be contamination from incomplete removal of inner membrane or cytosolic components. In this analysis, the number of MS/MS scans matched to a particular protein is proportional to the protein's abundance in the sample, making this method semi-quantitative. Among these 400 proteins were 22 putative TonB-dependent receptors, 4 of which were of far greater abundance in the iron-limited group (Figure 5.2). These 4 TonB-dependent receptors were also identified as being highly upregulated upon iron starvation in the microarray analysis (Figure 3.6), and qRT-PCR (for TERTU_4055; Figure 4.2.A). A multitude of transporters and other machinery that may be involved in iron acquisition was also identified (Figure 5.2).

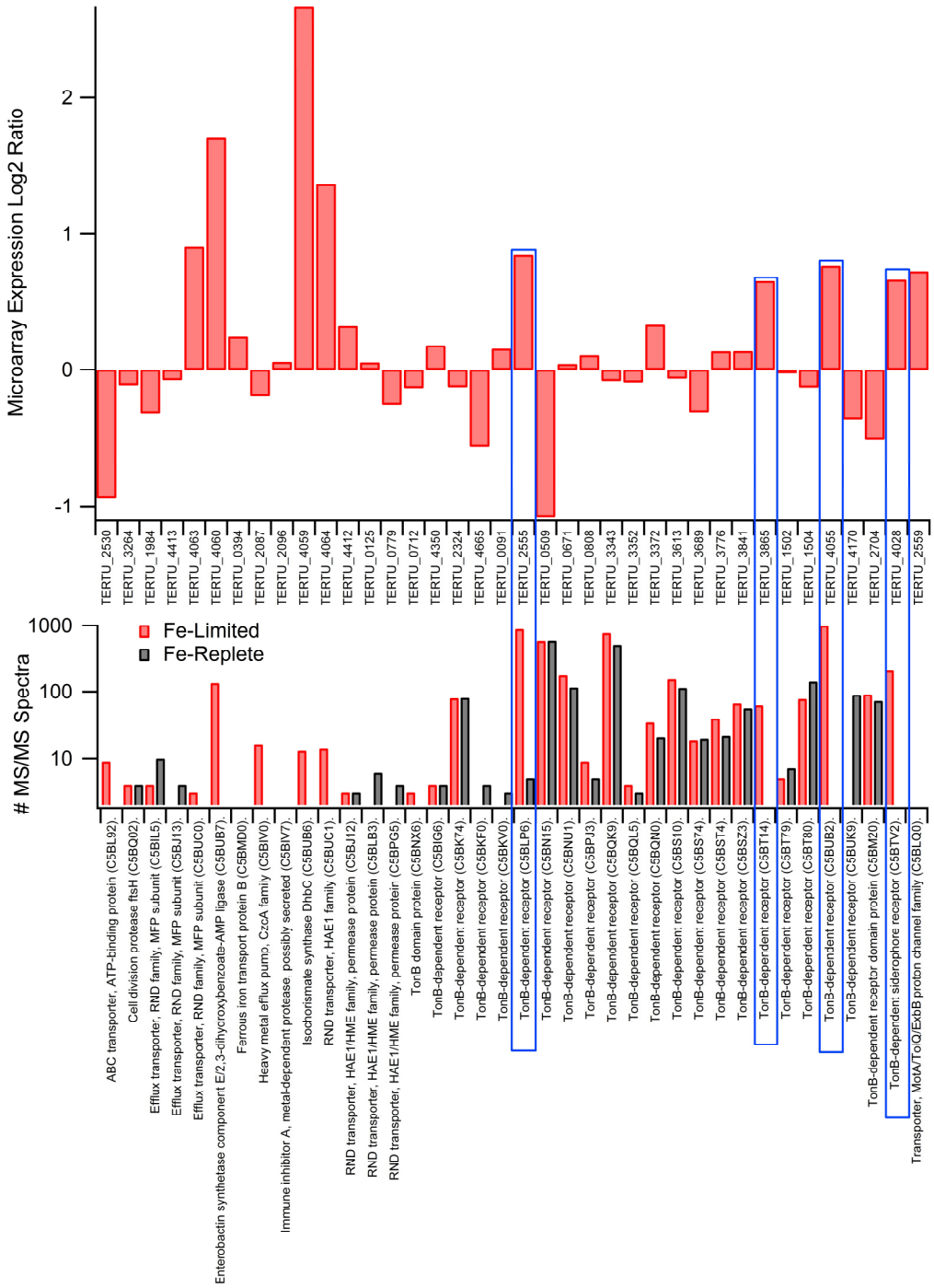

Figure 5.2 Relative quantitation of *T. turnerae* OM proteins from iron-replete and iron-limited cultures by LC-MS/MS. Shown is the number of MS/MS spectra of some of the putative TonB-dependent receptors and other proteins possibly involved in iron acquisition (bottom graph), along with the respective relative expression value from the microarray study (top graph). Boxed in blue are 4 putative TonB-dependent receptors that were highly upregulated in the microarray analysis (and qRT-PCR for TERTU_4055), and of far greater abundance in the OM of iron starved cells.

Collectively, these analyses (microarray and qRT-PCR expression profiling, CAS assay, and LC-MS/MS) provide strong evidence of which gene cluster is responsible for the biosynthesis and secretion of a siderophore in *T. turnerae*, as well as a possible ferric-siderophore uptake and utilization system. These studies have also demonstrated that the components of this iron acquisition system are regulated by iron availability, and have optimized culture conditions for targeted expression of the siderophore for purification, further characterization, and development of possible biotechnological applications.

Chapter 6

Assays for Bioactive Metabolites in *T. turnerae* Culture Extracts and Identification of Potential Fungal Targets

6.1 Introduction

Due to the large portion of the *T. turnerae* genome dedicated to producing secondary metabolites and the homology some of the secondary metabolite clusters share with known producers of bioactive natural products, looking for bioactive molecules in *T. turnerae* culture extracts is well-warranted. In fact, disc diffusion bioassays of *T. turnerae* crude culture extracts have shown both antibacterial and antifungal activity, although the culture conditions that result in the greatest activity have remained unclear (Figure 6.1).

(A) (B)

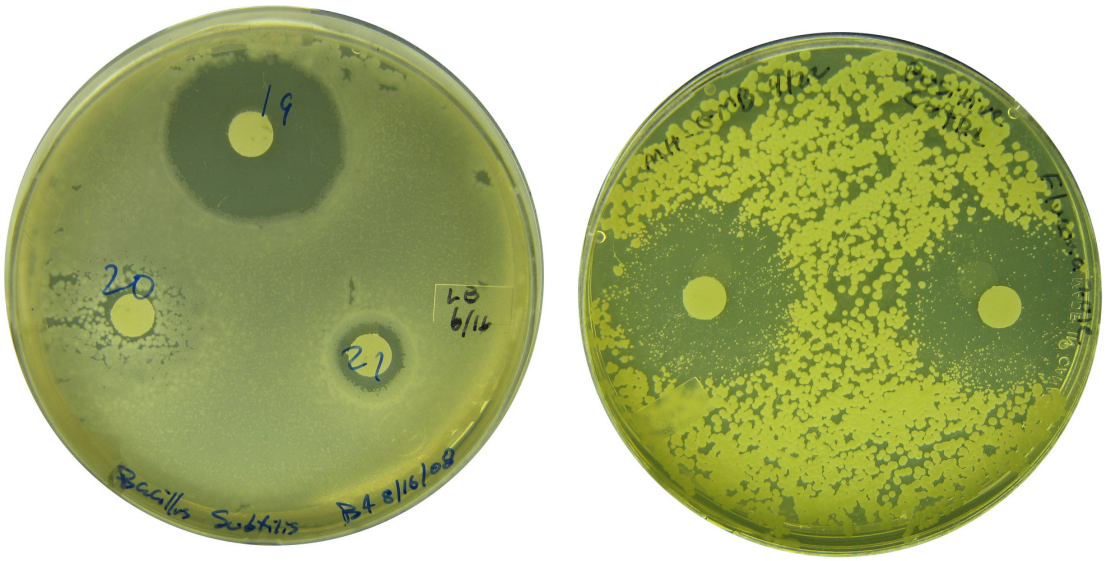

Figure 6.1 Disc diffusion bioassays of *T. turnerae* crude culture extracts reveal that it produces compounds that inhibit the growth of (A) *Bacillus subtilis* and (B) *Candida albicans*.

After observing striking transcriptional regulation of secondary metabolite genes exerted by P_i-availability from microarray (Chapter 3) and qRT-PCR (Chapter 4) analyses, it piqued my curiosity of whether the products produced by these gene clusters were biologically active.

Moreover, an interesting phenomenon in our *Lyrodus pedicellatus* shipworm aquaculture pointed out by Dan Distel provided the opportunity to characterize some of the potential targets of *T. turnerae* secondary metabolites. It was observed that fungi were growing on the same wood that harbored *L. pedicellatus*, but the fungal growth appeared to be confined to the opposite end of the wood from where the shipworm resided. It was hypothesized that this restriction of fungal growth may be due to antifungal metabolites secreted by the symbiont community in the shipworm (Figure 6.2).

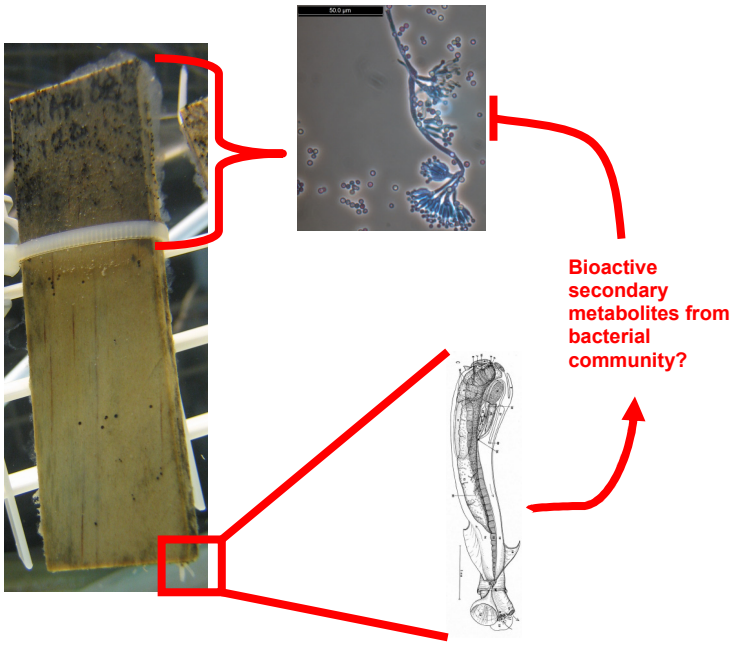

Figure 6.2 Model of fungal growth inhibition imposed by secondary metabolites produced by the shipworm symbiont community. Image on the left shows a plank of wood in aquaculture with external fungal growth restricted to the top portion, and the shipworm's siphons are boxed in red at the bottom portion.

This aquaculture system serves as a microcosm for the shipworm's natural environment, where there is stark competition for space and resources (e.g. cellulose), and allowed for the isolation and characterization of possible competitors of the shipworm and its bacterial symbionts.

6.2 Materials and Methods

Bacterial and fungal strains and culture conditions

Bacillus subtilis JH642 was kindly provided by Michiko Nakano (Oregon Health & Science University), and used to prepare a spore suspension for disc diffusion bioassays of antibacterial activity. Sporulation of *B. subtilis* was induced as described by Jenkinson *et al.* (1981), and spores were purified by repeated washing and centrifugation (Harwood, 1990). *B. subtilis* spores were routinely germinated at 30°C on lysogeny medium (pH 7.4) (Bertani, 1951) containing 10g tryptone (Sigma-Aldrich T2559), 5g yeast extract (Sigma-Aldrich 92144), 10g NaCl (Fisher BP358), and 1.5% (w:v) agar per liter, the same medium used for assaying general antibacterial activity of extracts by disc diffusion.

Candida albicans was obtained from the American Type Culture Collection (ATCC 90028), routinely grown at 37°C on potato dextrose agar (pH 5.6) (Sigma-Aldrich 70139), and was used to assay general antifungal activity of extracts.

Preparation of *T. turnerae* crude culture extracts and assay for bioactive metabolites

T. turnerae liquid cultures were transferred from the culture flask to 50mL Falcon tubes, and frozen at -80°C. Frozen cultures were concentrated by lyophilization, and the dry powder was extracted three times with methanol/chloroform (1:1) using the same solvent volume as the initial culture for each of the three extractions. Extracts were filtered over desiccant (anhydrous $Na_2S_2O_3$) through a Whatman #1 filter paper. The solvent was evaporated to dryness, and the resultant extract was weighed. Dry extracts were stored at -20°C.

Disc diffusion assays were performed by dissolving the dry, crude culture extracts in methanol/chloroform (1:1) and aliquoting 20µL of extract to a 6mm blank test disc (BD Diagnostic Systems 231039). Dry extracts from which a comparison was to be made were consistently reconstituted at the same dry weight:solvent ratio, resulting in the same final concentration of crude extract. Discs were air dried on a sterile microscope slide in a

laminar flow hood prior to being placed on a freshly-streaked lawn of test organism, *B. subtilis* or *C. albicans*, on the appropriate growth medium. Disc diffusion assays included an uninoculated medium extract to account for any growth inhibition of the test organism contributed by solvent impurities or components of the growth medium.

Isolation and phylogenetic analysis of fungi from *Lyrodus pedicellatus* aquaculture

Several *Lyrodus pedicellatus* shipworm specimens were kindly provided by Dan Distel (Ocean Genome Legacy) in planks of untreated wood and maintained in aquaculture with filtered seawater at ambient temperature. To isolate potential fungal targets of *T. turnerae* secondary metabolites, hyphae were scraped from the wood that inhabited *L. pedicellatus,* and transferred to SBM plates (see section 3.2 for description of medium). Aliquots of seawater from the aquarium were also streaked on SBM plates to germinate fungal spores suspended in the aquaculture. These fungal isolation plates were incubated either at 30°C or ambient temperature until growth was observed, and axenic cultures were obtained by repeated transfer of hyphae to fresh medium. Efforts were made to transfer hyphae to fresh media before any sporulation occurred on the mother fungal isolation plate, which would have made obtaining an axenic culture extremely difficult.

Fungal genomic DNA was extracted using a DNeasy® Plant Mini Kit (QIAGEN), and used as a template for PCR. The fungus-specific, universal primers ITS1 (5'-TCCGTAGGTGAACCTGCGG-3') and ITS4 (5'-TCCTCCGCTTATTGATATGC-3') were used for amplification of the rDNA internal transcribed spacer region (Innis, 1990). Amplicons were purified using a QIAquick® PCR Purification Kit (QIAGEN 28106), and sequenced. Amplicon sequence chromatograms were visualized in Finch TV (Geospiza) to verify that a single trace existed at each identified nucleotide, providing confidence the sequence is accurate and additional evidence that each amplicon was derived from an axenic culture. Sequences were aligned in ClustalW2 (Thompson *et al*., 1994) and edited using BioEdit (Hall, 1999) to minimize gaps and remove flanking sequences that did not align. From the edited multiple sequence alignment, a neighbor joining tree was constructed in MEGA (Kumar *et al*., 2008).

Co-plating bioassay for antifungal molecules produced by *T. turnerae*

A second type of bioassay was employed to assay antifungal activity using viable cells. *T. turnerae* was co-plated on SBM plates with a test organism in the manner depicted in Figure 6.3, and incubated at 30°C. An interruption in growth of the test organism centered around *T. turnerae* would qualify as a positive result.

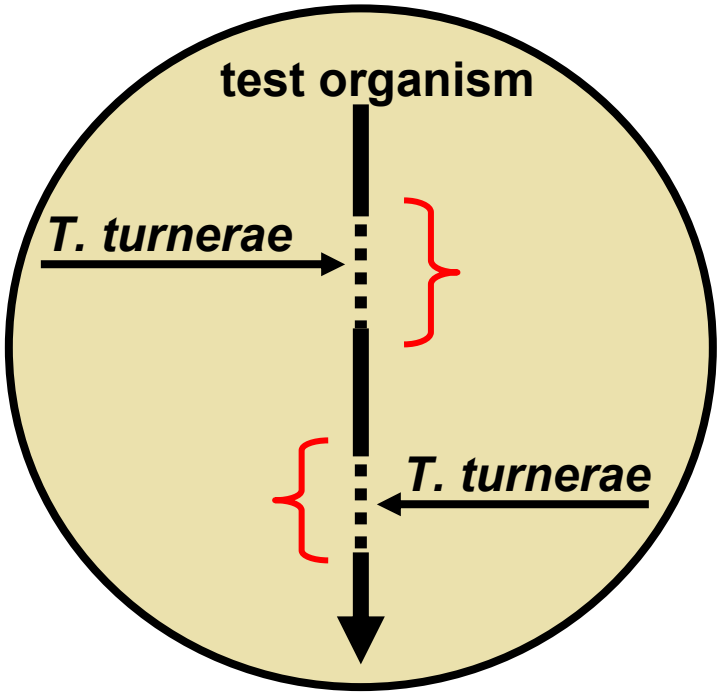

Figure 6.3 Depiction of a positive antimicrobial bioassay by co-plating technique. Growth interruptions of the test organism are indicated by red brackets.

6.3 Results and Discussion

Biosynthesis of an antibacterial molecule is regulated by phosphate availability

A disc diffusion assay of a 29hr P_i-limited crude methanol/chloroform *T. turnerae* extract showed significant inhibition of *B. subtilis* while the 29hr P_i-replete extract showed no inhibition (these are the same culture conditions from which RNA was prepared for microarray and qRT-PCR expression analysis), demonstrating that at least

one antibacterial molecule that inhibits growth of *B. subtilis* is regulated by P_i availability (Figure 6.4.A). The same extract that showed activity against *B. subtilis* did not show any activity against *C. albicans*, suggesting that the antibacterial and antifungal activities are attributed to at least two different molecules (Figure 6.4.B).

(A) (B)

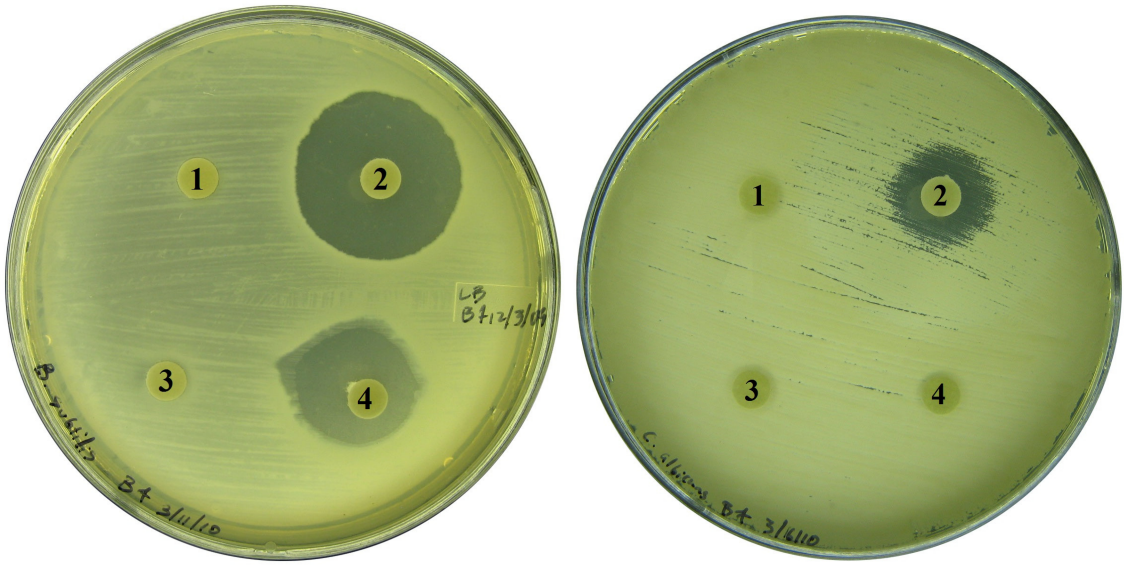

Figure 6.4 Disc diffusion bioassays of crude cellular extracts against (A) *B. subtilis* and (B) *C. albicans*. 1=uninoculated medium extract negative control; 2=ampicillin (for *B. subtilis*) or ketoconazole (for *C. albicans*) positive control; 3= P_i-replete culture extract; 4= P_i-limited culture extract.

The increased activity against *B. subtilis* seen in the P_i-limited crude extract implies that the biosynthesis of the molecule responsible for this activity is regulated by phosphate availability. Therefore, if this regulation is exerted at the transcriptional level, the gene cluster that produces this molecule would also be upregulated in P_i-limited conditions. Ergo, based on the microarray and qRT-PCR expression profiles of the secondary metabolite gene clusters, the most likely cluster responsible for the production of this antibacterial molecule is region 1.

The results of these bioassays show that *T. turnerae* produces multiple bioactive secondary metabolites, and in conjunction with the microarray and qRT-PCR expression analysis, it provides evidence of which gene cluster may be responsible for producing an

antibacterial molecule. This will facilitate targeted expression of the antibacterial molecule for purification and structure elucidation, and thus is one step towards possible discovery of a novel bioactive metabolite with pharmaceutical relevance.

Identification of potential fungal targets of *T. turnerae* secondary metabolites

To identify the fungi in our aquaculture that may be competing for resources and space with the shipworms (and thus potential targets of the symbiont secondary metabolites), seven genetically distinct fungi were isolated from this aquaculture, and identified by sequencing the rDNA internal transcribed spacer region (Figure 6.5.A). Three of these fungal isolates (FI) showed susceptibility to *T. turnerae* secondary metabolites when co-plated (FIs 5, 6, and 7; Figure 6.5.B). The isolates that showed this susceptibility grouped closely in the phylogenetic analysis. The four FIs that did not show susceptibility in the bioassay were all Penicillia, and were at a more shallow position in the neighbor-joining tree.

Growth of neither the FIs nor *C. albicans* was inhibited by disc diffusion assays of a pure *T. turnerae* compound that inhibited *B. subtilis* (data not shown; pure extract provided by Sherif Elshahawi, OHSU). This is in agreement with implications of the disc diffusion bioassay of a P_i-limited extract (Figure 6.4), which inhibited *B. subtilis* but not *C. albicans*, by suggesting that the antibacterial and antifungal activities observed are from at least two compounds. However, co-plating is a more dynamic assay than a disc diffusion style assay (which essentially provides a snapshot of the chemistry occurring at the time the extract is prepared), because it uses viable cells and allows the organisms to interact and respond to the presence of one another. One disadvantage to this assay is that the organisms must be able to grow on the same medium. The co-plating style bioassay was used with FIs because they grow efficiently on the same medium as *T. turnerae,* whereas growth of *C. albicans* and *B. subtilis* would be hindered due to the high salt concentration.

Examination of the wood in our aquaculture in which the shipworms reside showed no fungal growth on the exterior of the wood near the shipworm, although microscopic examination of the inside of the wood revealed the presence of fungal

hyphae (Figure 6.5.C). It is difficult to determine if this fungus inhabited the wood prior to the shipworm, or if it was still viable, but it stands to reason that the fungal community within this aquaculture shows varying degrees of susceptibility to the antifungal molecules produced by *T. turnerae*.

While it seems likely that the antifungal molecule(s) produced by *T. turnerae* would be a secondary metabolite(s), this is not necessarily so. For example, *T. turnerae* encodes a putative chitin binding protein (TERTU_0046) and chitinase (TERTU_0285) that could act on the chitin in fungal cell walls and inhibit their growth, even though enzymes for the degradation of the fungal polysaccharide pullulan are absent in *T. turnerae*. Also secreted by *T. turnerae* are considerable amounts of organic acids such as succinic acid, acetic acid, and formic acid, which result in a significant decrease in pH of its growth environment. If a fungus is sensitive to these organic acids, or the low pH created by *T. turnerae* secreting them, this may also result in fungal growth inhibition. Another possibility is that the siderophore produced by *T. turnerae* for its own iron assimilation serves a secondary antimicrobial function by limiting iron from competitors. However, *T. turnerae* extracts that showed high activity in the CAS assay (and thus presumably had high siderophore concentrations) did not have any activity against *B. subtilis* or *C. albicans* (not shown), so it seems unlikely that this siderophore has antibacterial or antifungal roles.

(A)

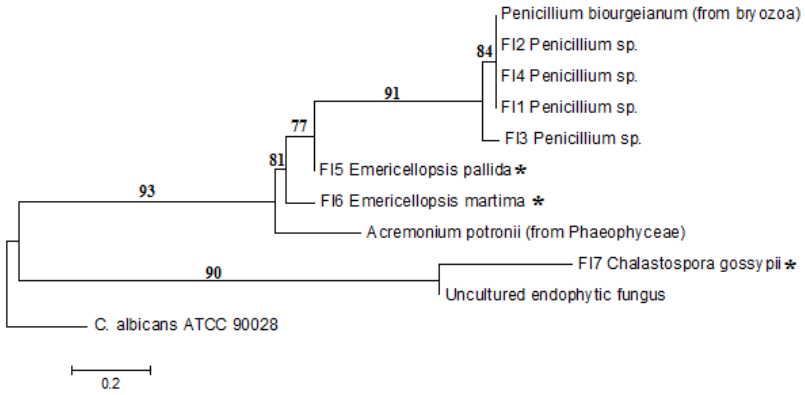

(B) FI5 FI6 FI7

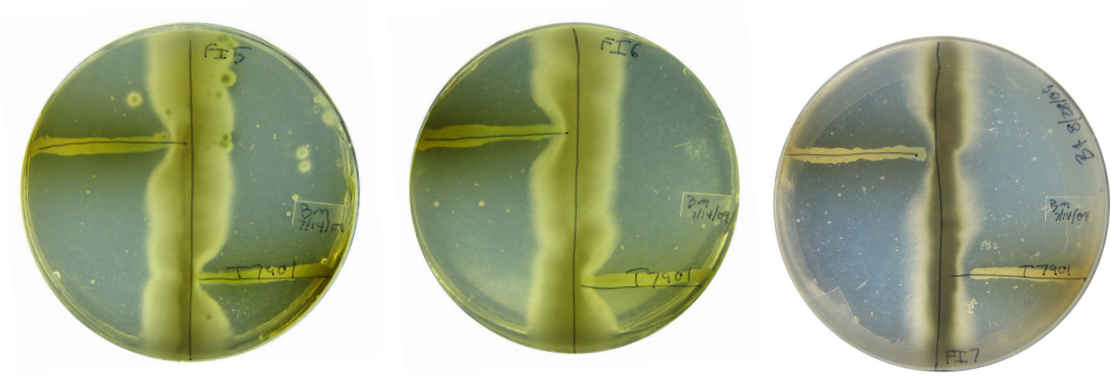

(C)

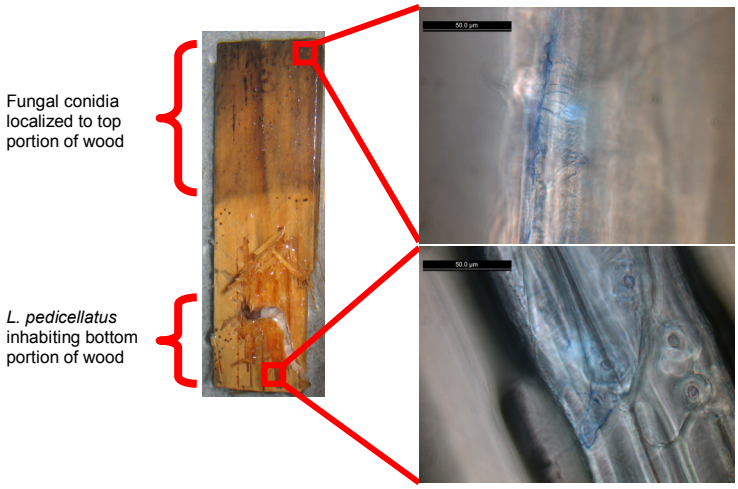

Figure 6.5 (A) Neighbor-joining phylogenetic tree based on fungal rDNA internal transcribed spacer sequences. The scale bar represents 0.2 substitutions per nucleotide position. Stars indicate the fungal isolates (FI) that showed susceptibility to *T. turnerae* metabolites in a co-plating bioassay. (B) Co-plating of three of the seven fungal isolates from *L. pedicellatus* aquaculture with *T. turnerae* shows they are susceptible to compounds secreted by *T. turnerae*. (C) Microscopic analysis using a chitin stain of the wood harboring *L. pedicellatus* revealed fungal hyphae (blue) in close proximity to the shipworm, even though there was no fungal growth on the external surface of the wood.

Currently, the role fungi play in shipworm symbioses and polysaccharide degradation is not clear. Often in nature there is cooperation between a consortium of organisms to fully degrade lignocellulosic material. White rot fungi, including Ascomycota and Basidiomycota, are known for their distinguished ability to degrade lignin (Leonowicz, 1999), while soft rot and brown rot fungi tend to prefer wood carbohydrates and modify lignin to a limited extent (Tien & Kirk, 1988). *T. turnerae* lacks the enzymatic machinery to degrade lignin, so perhaps it would welcome the presence of white rot fungi to degrade lignin and provide it better access to plant cell wall polysaccharides. In this manner, it is conceivable that there is a division of labor between the bacterial symbiont community within the shipworm and fungi in the external environment to cooperatively degrade complex polysaccharides. On the other hand, it may dissuade soft rot and brown rot fungi, which may be directly competing with shipworms for cellulose, by producing antifungal molecules specifically tailored to inhibit their growth.

Chapter 7

Conclusions

Gene expression data (microarray and qRT-PCR) discussed here have identified iron-regulated elements in the *T. turnerae* T7901 genome that may be responsible for the biosynthesis, secretion, uptake, and hydrolysis of a catecholate-like siderophore. These data provide evidence that the genomic region primarily responsible for iron transport is localized to secondary metabolite region 7. MS analysis of OM proteins corroborated the expression data by identifying the same putative siderophore receptors to be of far greater abundance in the membranes of cells subjected to iron-limiting conditions, as were found to be upregulated in the same conditions in the expression analysis. The CAS assay chemically confirmed the presence of iron chelating molecules in the iron-limited culture supernatant, which were absent in the iron-replete culture supernatant, providing chemical evidence for the presence of the siderophores. This study facilitates future genetic studies by providing evidence of which genes produce each component of the siderophore-mediated iron acquisition system in *T. turnerae*. The optimized iron-limited growth medium, and demonstration that the siderophore system is iron-regulated, allows us to target overexpression of these genes for further characterization of this siderophore and possible development of applications such as siderophore-mediated drug delivery.

The expression data (microarray and qRT-PCR) also suggested a phosphate regulation system is in place for at least one of the putative secondary metabolite gene clusters, region 1. From the disc diffusion bioassay we observed that phosphate availability also regulates the production of an antibacterial molecule that inhibits the growth of *B. subtilis*, so it is likely that the gene product of region 1 is responsible for this activity. The PKS and NRPS in region 1 share about 50% sequence similarity to that of *Bacillus amyloliquefaciens*, and the other half of the sequence does not match any sequences in the BLAST database. This extent of homology is likely to result in some

structural and biochemical similarities, yet different enough to promise a novel compound that may possess a unique biological activity. The optimized P_i-limited growth medium, and demonstration that production of the antibacterial molecule is P_i-regulated at the transcriptional level, allows us to target overexpression of this molecule for further characterization in anticipation of novel drug discovery.

Although the biosynthetic regulation of an antifungal molecule remained elusive throughout this study, disc diffusion and co-plating assays confirmed that *T. turnerae* has antifungal capabilities. Furthermore, extracts that inhibited *B. subtilis* did not possess antifungal activity, suggesting that the antibacterial and antifungal activities are from at least two distinct molecules. Further characterization of the biosynthetic regulation and structure of this antifungal molecule(s) is a potential area for future work.

Secondary metabolite region 2 sparked interest by showing some extent of regulation by phosphate availability, but the data for this region remain inconclusive. The three PKS genes (required for the biosynthesis of the final product of this region) did not show a clear phosphate regulation pattern, and only part of the starter unit (the malonyl CoA-ACP-transacylase) was P_i-regulated, suggesting that this cluster is not actively manufacturing its gene product.

Much of this work focused on only three of the nine putative secondary metabolite regions (1, 2 and 7), so there is far more territory to be explored in the secondary metabolome of this organism.

Microarray expression analysis of the carbohydrate-active genes showed a surprising expression pattern, in that many of these genes were expressed at comparable levels in cellulosic and sucrose-based media. This "constitutive" expression of the carbohydrate-active genes may be due to the insolubility of substrate (and that *T. turnerae* lacks a direct substrate detection method), or the physical partition between the bacteriocytes that harbor the symbionts and the digestive tract of the host through which the substrate passes. Nonetheless, the notion that *T. turnerae* will produce its carbohydrate-active enzymes in the absence of cellulose suggests that a sucrose-based (and thus more efficient and economical) system for enzyme production can be developed for biofuel applications.

Although work with *T. turnerae* T7901 began more than three decades ago, our understanding of its diverse physiological roles in the shipworm symbiosis is just beginning to coalesce. The scope of the work presented here is undoubtedly broad, but the topics become unified to a single theme in that they pertain to the essential physiological role of *T. turnerae* in its symbiosis, and show promise of biotechnological applicability: siderophore-mediated drug delivery, discovery of novel antibacterial and antifungal molecules, and development of biofuels are all within the scope of this work. Prior work with bacterial symbionts of shipworms has been centered on the nutritional role of the symbionts; a topic discussed here as well, although the greatest novel contribution of this work is the exploration of the role of *T. turnerae* secondary metabolites in chemical defense, and the progress towards developing applications of these molecules.

Appendix A

An Alternative Growth Medium for *T. turnerae* Results in Significant Physiological Changes

A.1 Introduction

An alternative basal medium (called ABM here) for *T. turnerae* was initially described by Greene and Freer in 1986, and since that time the composition has been repeatedly modified (Trindade-Silva *et al*., 2009; Ferreira *et al*., 2001; Ahuja *et al*., 2004). When grown in ABM, *T. turnerae* presents a drastically different morphology from what is seem in SBM, and is associated with increased secretion of extracellular protease and a decrease in endoglucanase activity (Ferreira *et al*., 2001).

ABM was used for here for preliminary physiological experiments prior to optimization of SBM (described in section 3.2), and some of these results are described.

A.2. Materials and Methods

T. turnerae culture conditions

ABM was prepared to result in the following per liter of ultrapure water: NaCl, 18.8g; KCl, 0.4g; $MgSO_4 \cdot 7H_20$, 1.9g; $MgCl_2 \cdot 6H_20$, 1.5g; $CaCl_2 \cdot 2H_20$, 0.4g; HEPES, 4.9g (unless otherwise indicated); NH_4Cl, 1g; sucrose or carboxymethylcellulose (CMC) (Sigma C9481), 5g; solution A, 10ml; solution B, 1ml. Solution A consisted of the following per liter of ultrapure water: $K_2HPO_4 \cdot 3H_20$, 24.0g; Na_2CO_3, 12.0g; $Fe_2(SO_4)_3$, 0.3g. Solution B consisted of the following per liter of deionized water: H_3BO_3, 2.9g; $MnCl_2 \cdot 4H_20$, 21.6g (unless otherwise indicated); $ZnSO_4 \cdot 7H_20$, 0.2g; $Na_2MoO_4 \cdot 2H_20$,

0.04g; $CoSO_4 \bullet 7H_20$, 0.05g; $CuSO_4 \bullet 5H_20$, 0.04g. After autoclaving, the pH was adjusted to 8.0 with sterile 1M NaOH. The carbon and nitrogen source were autoclaved separate from the salt solution, as were solutions A and B, and the four solutions were mixed aseptically immediately before use.

Culture supernatants were assayed for the presence of siderophores by the chrome azurol sulfonate (CAS) assay, and microarray expression analysis was performed as described in section 3.2.

A.3. Results and Discussion

A *T. turnerae* morphology transition is medium-dependent

In liquid ABM, *T. turnerae* assumes a different morphology from what is seen in SBM; an aggregated, benthic morphology is characteristic of growth in ABM and a rod-shaped, planktonic morphology is seen in SBM. Also, a spectrum of pigments are produced in ABM that are largely absent in SBM (Figure A.1.).

(A)

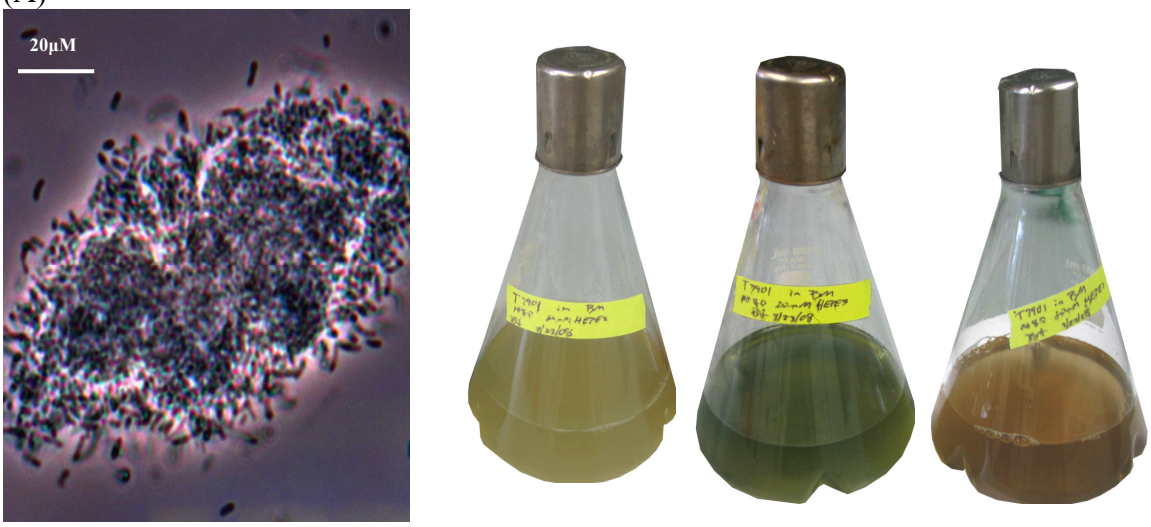

(B)

Figure A.1 (A) *T. turnerae* assumes an aggregated morphology in ABM (left) and produces various pigments throughout its growth in liquid culture (right). (B) *T. turnerae* grows planktonically in SBM (left) and cultures are opaque, except for in iron-limited conditions (left flask is an iron-replete culture; right flask is iron-limited).

Iron limitation in ABM induces siderophore biosynthesis in *T. turnerae*

The iron source in ABM is an inorganic, non-chelated form ($Fe_2[SO_4]_3$), and insoluble at the initial pH of 8.0 of the growth medium. Because the iron is essentially unavailable, *T. turnerae* becomes starved of iron and the siderophore-mediated iron acquisition system is stimulated. The CAS activity of ABM supernatant was similar to

that seen in iron-limited SBM (Figure A.2), and preliminary data show that the color phenomenon seen in ABM is attributed to siderophore activity. Elimination of Mn from ABM resulted in the complete absence of green pigmentation (not shown; the culture had the same opacity as SBM) and more detectable CAS activity. When Mn was then added (to match the concentration of standard ABM described in section A.2) to the -Mn ABM supernatant that had high CAS activity, a green color emerged, and the detectable CAS activity decreased (Figure A.2). The mechanism of the CAS assay (Figure 3.1) only allows for detection of unbound (deferrated) siderophores, so if the siderophores in the -Mn ABM are in fact interacting with the Mn that is added, the CAS activity would be expected to decrease.

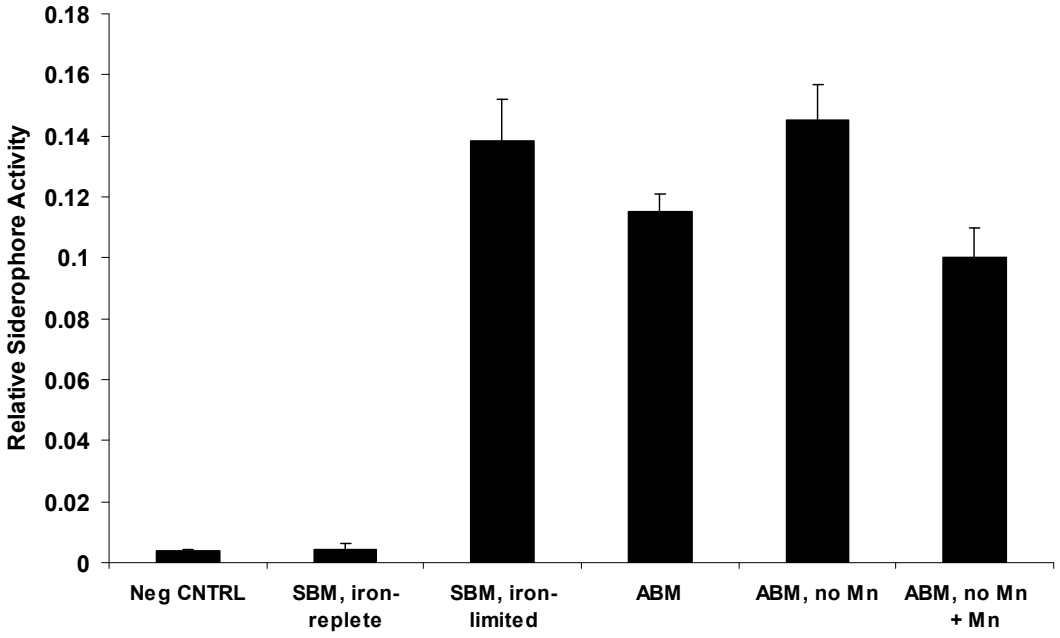

Figure A.2 CAS assay of supernatants from *T. turnerae* SBM and ABM. ABM has a comparable level of CAS activity as iron-limited SBM, and this activity is even greater in ABM without added Mn. Supplementation of Mn to the -Mn ABM supernatant results in a decrease in CAS activity, possibly suggesting the siderophore is binding the Mn, and is no longer detectable by this assay.

Expression of secondary metabolite genes is altered in ABM

Microarray expression analysis of secondary metabolite genes showed significant differences between cells grown in ABM and SBM (Figure A.3). In agreement with the CAS assay results (Figure A.2), the siderophore biosynthetic gene cluster (secondary metabolite region 7) was upregulated in ABM relative to SBM.

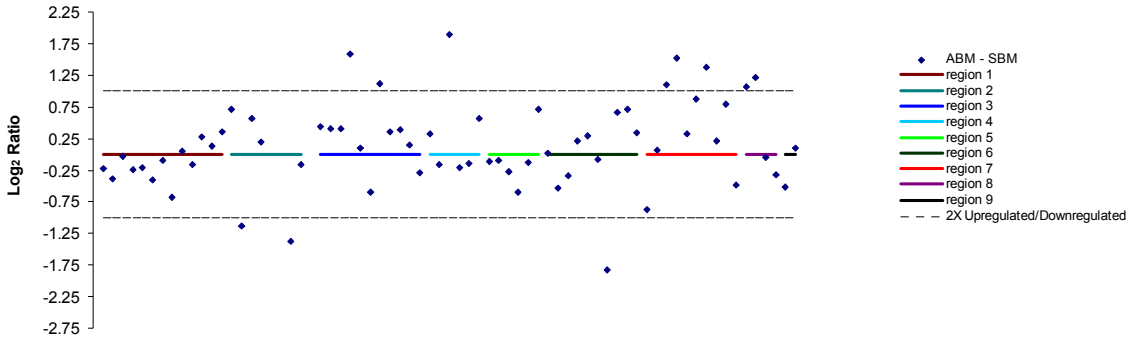

Figure A.3 Expression comparison of *T. turnerae* secondary metabolite genes in ABM and SBM. Data points represent the $\log_2$ ratio of the ABM to SBM normalized signal intensities. Each point represents one gene, and the secondary metabolite region of a given gene is indicated by the color of the x axis. Regions 3 and 7 showed the greatest extent of upregulation in ABM.

Frequently, crude culture extracts from ABM have greater antifungal activity than those from SBM (not shown), so this comparative expression analysis (Figure A.3) may provide evidence of which gene cluster(s) is responsible for the production of an antifungal molecule(s). As a result of the upregulation of region 3 in ABM, future studies on the biosynthesis and regulation of the antifungal molecule(s) could begin with this region. However, an unidentified precipitate is often observed in ABM, so the actual composition of this medium is less defined than SBM, and thus complicates the interpretation of expression data.

Carboxymethylcellulose is an acid-free substrate in ABM

Significant organic acid production was observed in ABM, resulting in a decrease from 8.0 to around 5.5 after several days of growth. This pH change can be mitigated by

increasing the HEPES concentration from 20mM to 100mM or substituting carboxymethylcellulose (CMC) for sucrose as the sole carbon source (Figure A.4.A). CMC is a sodium salt derivative (and thus is water-soluble) of cellulose that has carboxymethyl groups (-CH_2-COONa) bound to some of the hydroxyl groups of the glucopyranose monomers that make up the cellulose backbone (Figure A.4.B). Degradation of sucrose or cellulose is conducive to organic acid production due to the hydroxyl groups on the backbone, but the substitution of carboxymethyl groups for these hydroxyl groups largely abates the formation of the organic acids.

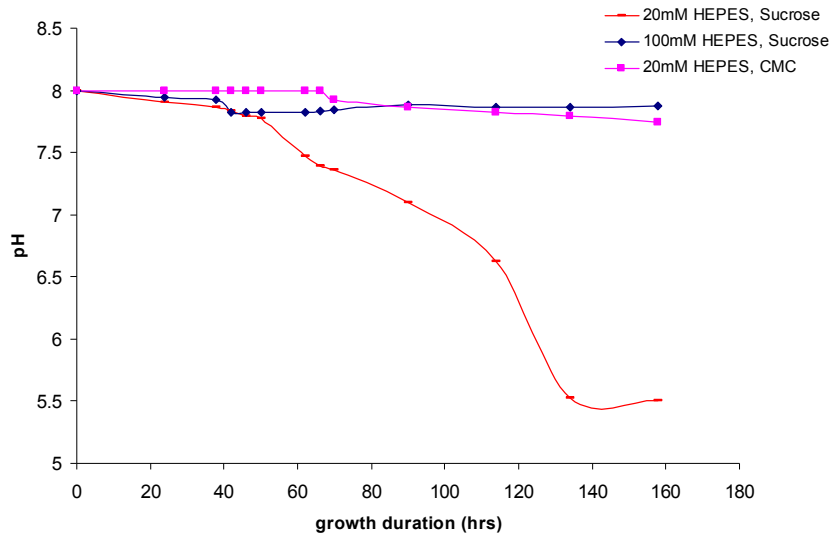

(B) Sucrose Cellulose CMC

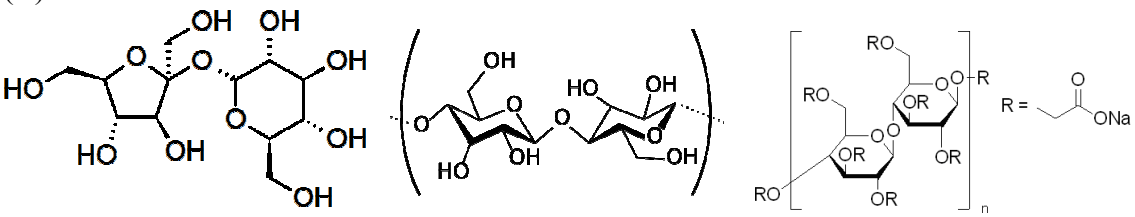

Figure A.4 (A) pH of ABM liquid culture showed a substantial decrease with 20mM HEPES and sucrose as the carbon source (red line). Increasing the buffer concentration to 100mM HEPES (blue line), or using CMC in place of sucrose (pink line) reduces the extent of pH reduction. (B) Structures of sucrose, cellulose, and CMC, an essentially acid-free substrate due to the substitution of carboxymethyl groups for hydroxyl groups present in sucrose and cellulose.

A comparison of *T. turnerae* growth kinetics in SBM and ABM

Analyzing the growth kinetics of *T. turnerae* in the aggregated morphology presents a challenge, because the conventional methods of optical density measurement or colony counts cannot be used due to the culture heterogeneity resulting from aggregate formation. For this reason, extracellular protein quantitation was used here. For proof of principle, a detailed growth curve of SBM static growth (no agitation) in a 48-well format showed extremely high reproducibility, and provided additional assurance that optical density measurements in SBM are accurate and precise (Figure A.5.A). Comparing the growth curves of SBM and ABM show that lag phase is prolonged in ABM (Figure A.5.B).

(A)

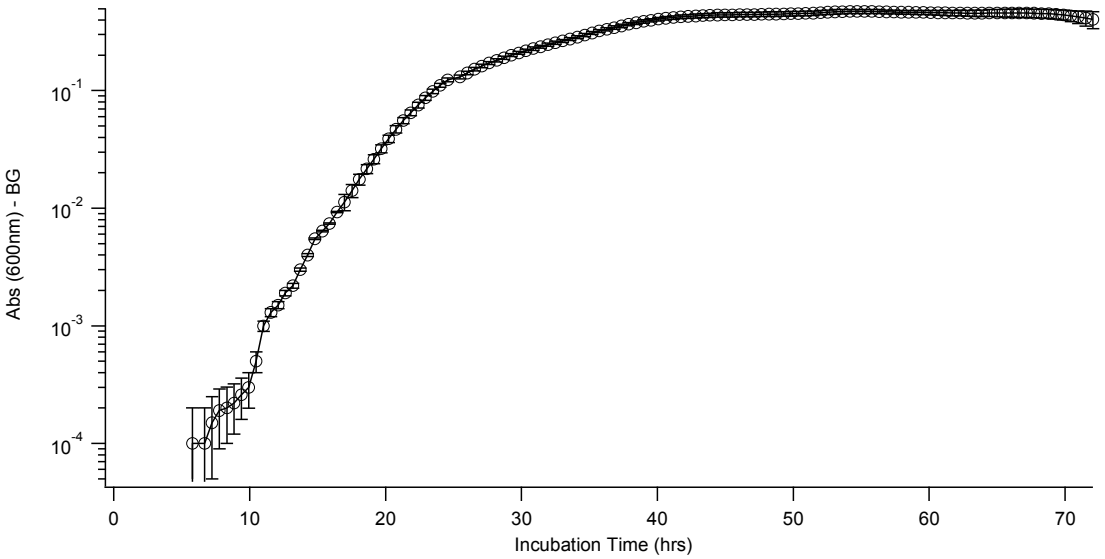

(B)

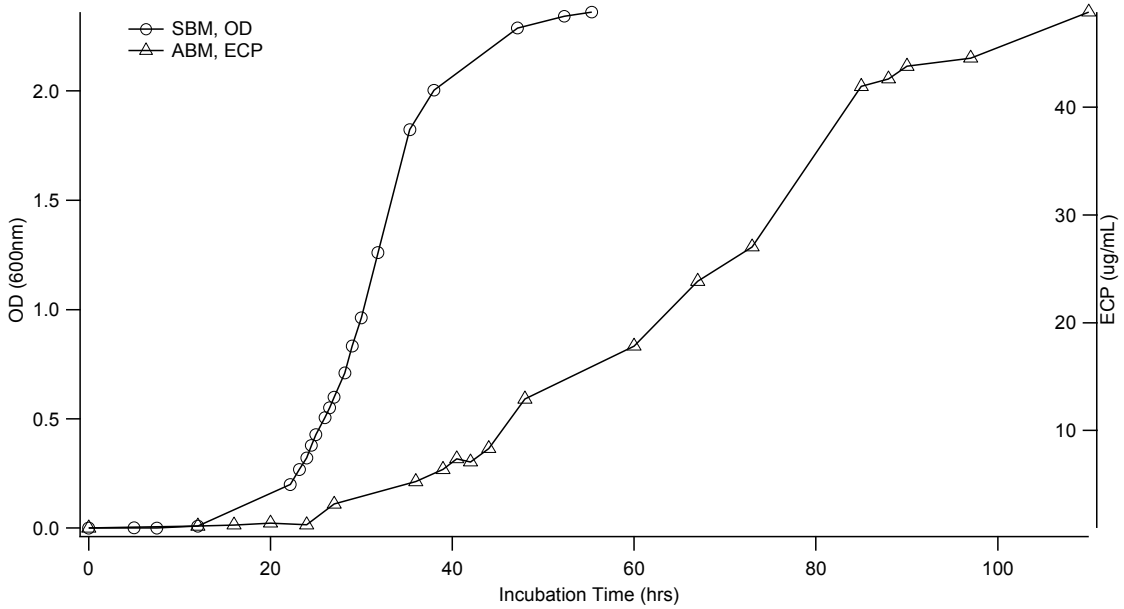

Figure A.5 (A) Optical density of *T. turnerae* static growth in SBM. An autoread well scan option was used, which recorded nine OD readings from different parts of each well, for each time increment. Shown here is the average of the 324 reads per time increment ([48 wells - 12 uninoculated control wells] x 9 reads/well = 324 reads per time increment). Error bars indicate one standard deviation. (B) Comparison of *T. turnerae* growth in SBM (circles) and ABM (triangles) with sucrose as the carbon source and 20mM HEPES. These cultures were grown at 30°C, 125RPM.

References

Ahmer, B.M. et al., 1995. Characterization of the exbBD operon of Escherichia coli and the role of ExbB and ExbD in TonB function and stability. *Journal of bacteriology*, 177(16), 4742.

Ahuja, S.K., Ferreira, G.M. & Moreira, A.R., 2004a. Application of Plackett-Burman design and response surface methodology to achieve exponential growth for aggregated shipworm bacterium. *Biotechnology and Bioengineering*, 85(6), 666-675.

Ahuja, S.K., Ferreira, G.M. & Moreira, A.R., 2004b. Production of an endoglucanase by the shipworm bacterium, Teredinobacter turnirae. *Journal of Industrial Microbiology and Biotechnology*, 31(1), 41-47.

Alduina, R. et al., 2007. Phosphate-Controlled Regulator for the Biosynthesis of the Dalbavancin Precursor A40926. *Journal of Bacteriology*, 189(22), 8120-8129.

Alper, H. & Stephanopoulos, G., 2009. Engineering for biofuels: exploiting innate microbial capacity or importing biosynthetic potential? *Nature Reviews Microbiology*, 7(10), 715-723.

Althaus, E.W. et al., 1999. The ferric uptake regulation (Fur) repressor is a zinc metalloprotein. *Biochemistry*, 38(20), 6559-6569.

Anbar, A.D. & Knoll, A.H., 2002. Proterozoic Ocean Chemistry and Evolution: A Bioinorganic Bridge? *Science*, 297(5584), 1137-1142.

Anderson, C.R. et al., 2009. Mn(II) Oxidation Is Catalyzed by Heme Peroxidases in "Aurantimonas manganoxydans" Strain SI85-9A1 and Erythrobacter sp. Strain SD-21. *Applied and Environmental Microbiology*, 75(12), 4130-4138.

Anderson, T.B., Brian, P. & Champness, W.C., 2001. Genetic and transcriptional analysis of absA, an antibiotic gene cluster-linked two-component system that regulates multiple antibiotics in Streptomyces coelicolor. *Molecular Microbiology*, 39(3), 553–566.

Archibald, F., 1983. Lactobacillus plantarum , an organism not requiring iron. *FEMS Microbiology Letters*, 19(1), 29-32.

Arguelles-Arias, A. et al., 2009. Bacillus amyloliquefaciens GA 1 as a source of potent antibiotics and other secondary metabolites for biocontrol of plant pathogens. *Microbial Cell Factories*, 8(1), 63.

Balado, M., Osorio, C.R. & Lemos, M.L., 2006. A gene cluster involved in the

biosynthesis of vanchrobactin, a chromosome-encoded siderophore produced by Vibrio anguillarum. *Microbiology*, 152(12), 3517.

Balado, M., Osorio, C.R. & Lemos, M.L., 2008. Biosynthetic and regulatory elements involved in the production of the siderophore vanchrobactin in Vibrio anguillarum. *Microbiology*, 154(5), 1400.

Balado, M., Osorio, C.R. & Lemos, M.L., 2009. FvtA Is the Receptor for the Siderophore Vanchrobactin in Vibrio anguillarum: Utility as a Route of Entry for Vanchrobactin Analogues. *Applied and Environmental Microbiology*, 75(9), 2775-2783.

Bentley, S.D. et al., 2002. Complete genome sequence of the model actinomycete Streptomyces coelicolor A3(2). *Nature*, 417(6885), 141-147.

Bertani, G., 1951. Studies on lysogenesis. I. The mode of phage liberation by lysogenic Escherichia coli. *J Bacteriol*, 62(3), 293–300.

Bilban, M. et al., 2002. Normalizing DNA microarray data. *Current Issues in Molecular Biology*, 4, 57–64.

Binder, J.B. & Raines, R.T., 2010. Fermentable sugars by chemical hydrolysis of biomass. *Proceedings of the National Academy of Sciences*, 107(10), 4516.

Bingle, L.E., Bailey, C.M. & Pallen, M.J., 2008. Type VI secretion: a beginner's guide. *Current Opinion in Microbiology*, 11(1), 3-8.

Bradford, M.M. & others, 1976. A rapid and sensitive method for the quantitation of microgram quantities of protein utilizing the principle of protein-dye binding. *Analytical biochemistry*, 72(1-2), 248–254.

Braun, U. et al., 2003. Phylogeny and taxonomy of Cladosporium-like hyphomycetes, including Davidiella gen. nov., the teleomorph of Cladosporium s. str. *Mycological Progress*, 2(1), 3–18.

Breznak, J.A. & Brune, A., 1994. Role of microorganisms in the digestion of lignocellulose by termites. *Annual Review of Entomology*, 39(1), 453–487.

Bsat, N. et al., 1998. Bacillus subtilis contains multiple Fur homologues: identification of the iron uptake (Fur) and peroxide regulon (PerR) repressors. *Molecular Microbiology*, 29(1), 189-198.

Bull, C.T., Ishimaru, C.A. & Loper, J.E., 1994. Two genomic regions involved in catechol siderophore production by Erwinia carotovora. *Applied and Environmental Microbiology*, 60(2), 662.

Butler, M.S., 2005. Natural products to drugs: natural product derived compounds in clinical trials. *Natural Product Reports*, 22(2), 162.

Carpita, N.C. & Gibeaut, D.M., 1993. Structural models of primary cell walls in flowering plants: consistency of molecular structure with the physical properties of the walls during growth. *The Plant Journal: For Cell and Molecular Biology*, 3(1), 1-30.

Cheng, Y.Q., Tang, G.L. & Shen, B., 2003. Type I polyketide synthase requiring a discrete acyltransferase for polyketide biosynthesis. *Proceedings of the National Academy of Sciences*, 100(6), 3149.

Chuaqui, R.F. et al., 2002. Post-analysis follow-up and validation of microarray experiments. *Nature genetics*, 32(supp), 509–514.

Clarke, A., 1996. *Biodegradation of cellulose : enzymology and biotechnology*, Lancaster Pa.: Technomic Pub. Co.

Coderre, P.E. & Earhart, C.F., 1989. The entD gene of the Escherichia coli K12 enterobactin gene cluster. *Journal of General Microbiology*, 135(11), 3043-3055.

Cosgrove, D.J., 2005. Growth of the plant cell wall. *Nature Reviews Molecular Cell Biology*, 6(11), 850–861.

Cowling, E.B. & Merrill, W., 1966. Nitrogen in wood and its role in wood deterioration. *Botany*, 44(11), 1539-1554.

Crawford, J.M. et al., 2006. Identification of a starter unit acyl-carrier protein transacylase domain in an iterative type I polyketide synthase. *Proceedings of the National Academy of Sciences*, 103(45), 16728.

Crosa, J.H. & Hodges, L.L., 1981. Outer membrane proteins induced under conditions of iron limitation in the marine fish pathogen Vibrio anguillarum 775. *Infection and immunity*, 31(1), 223.

Crous, P.W. et al., 2009. Phylogeny and taxonomy of obscure genera of microfungi. *Persoonia-Molecular Phylogeny and Evolution of Fungi*, 22(1), 139–161.

Dansen, T.B. & Wirtz, K.W., The peroxisome in oxidative stress. *The Role of Peroxisomes in Oxidative Stress*, 20.

Davidson, S.K. et al., 2001. Evidence for the biosynthesis of bryostatins by the bacterial symbiont" Candidatus Endobugula sertula" of the bryozoan Bugula neritina. *Applied and Environmental Microbiology*, 67(10), 4531.

Deutscher, M.P., 2006. Degradation of RNA in bacteria: comparison of mRNA and

stable RNA. *Nucleic acids research*, 34(2), 659.

Distel, 2002. *Wood deterioration and preservation : advances in our changing world* American Chemical Society., ed., Washington DC: American Chemical Society.

Distel, D.L., Beaudoin, D.J. & Morrill, W., 2002. Coexistence of multiple proteobacterial endosymbionts in the gills of the wood-boring bivalve Lyrodus pedicellatus (Bivalvia: Teredinidae). *Applied and Environmental Microbiology*, 68(12), 6292.

Distel, D.L. et al., 1988. Sulfur-oxidizing bacterial endosymbionts: analysis of phylogeny and specificity by 16S rRNA sequences. *Journal of bacteriology*, 170(6), 2506.

Distel, D.L. et al., 2002. Teredinibacter turnerae gen. nov., sp. nov., a dinitrogen-fixing, cellulolytic, endosymbiotic gamma-proteobacterium isolated from the gills of wood-boring molluscs (Bivalvia: Teredinidae). *International Journal of Systematic and Evolutionary Microbiology*, 52(6), 2261.

Distel, D.L. & Roberts, S.J., 1997. Bacterial endosymbionts in the gills of the deep-sea wood-boring bivalves Xylophaga atlantica and Xylophaga washingtona. *The Biological Bulletin*, 192(2), 253.

Donadio, S., Sosio, M. & Lancini, G., 2002. Impact of the first Streptomyces genome sequence on the discovery and production of bioactive substances. *Applied Microbiology and Biotechnology*, 60(4), 377-380.

Dubois, M. et al., 1956. Colorimetric method for determination of sugars and related substances. *Analytical chemistry*, 28(3), 350–356.

Eisen, J.A., Smith, S.W. & Cavanaugh, C.M., 1992. Phylogenetic relationships of chemoautotrophic bacterial symbionts of Solemya velum say (Mollusca: Bivalvia) determined by 16S rRNA gene sequence analysis. *Journal of bacteriology*, 174(10), 3416.

Ekborg, N.A., 2005. Saccharophagus degradans gen. nov., sp. nov., a versatile marine degrader of complex polysaccharides. *International Journal of Systematic and Evolutionary Microbiology*, 55(4), 1545-1549.

Ekborg, N.A. et al., 2007. CelAB, a Multifunctional Cellulase Encoded by Teredinibacter turnerae T7902T, a Culturable Symbiont Isolated from the Wood-Boring Marine Bivalve Lyrodus pedicellatus. *Applied and Environmental Microbiology*, 73(23), 7785-7788.

Eriksson, K., 1990. *Microbial and enzymatic degradation of wood and wood components*, Berlin ;;New York: Springer-Verlag.

Escolar, L., Perez-Martin, J. & de Lorenzo, V., 1999. Opening the iron box:

transcriptional metalloregulation by the Fur protein. *Journal of bacteriology*, 181(20), 6223.

Ferguson, A.D. & Deisenhofer, J., 2002. TonB-dependent receptors—structural perspectives. *Biochimica et Biophysica Acta (BBA) - Biomembranes*, 1565(2), 318-332.

Ferreira, G.M. et al., 2001. Pleomorphism of the marine bacterium Teredinobacter turnirae. *Letters in Applied Microbiology*, 33(1), 56-60.

Filloux, A., Hachani, A. & Bleves, S., 2008. The bacterial type VI secretion machine: yet another player for protein transport across membranes. *Microbiology*, 154(6), 1570.

Fisch, K.M. et al., 2009. Polyketide assembly lines of uncultivated sponge symbionts from structure-based gene targeting. *Nature Chemical Biology*, 5(7), 494-501.

Forster, T., Roy, D. & Ghazal, P., 2003. Experiments using microarray technology: limitations and standard operating procedures. *Journal of Endocrinology*, 178(2), 195.

Gallager, S.M., Turner, R.D. & Berg, C.J.J., 1981. Physiological aspects of wood consumption, growth, and reproduction in the shipworm Lyrodus pedicellatus Quatrefages (Bivalvia: Teredinidae). | Gallager, S. M., Turner, R. D., Berg, C. J., Jr. | Journal of Experimental Marine Biology and Ecology |. Available at: http://www.cababstractsplus.org/ABSTRACTS/Abstract.aspx?AcNo=19811423937 [Accessed March 9, 2010].

Gil-Turnes, M.S., Hay, M.E. & Fenical, W., 1989. Symbiotic marine bacteria chemically defend crustacean embryos from a pathogenic fungus. *Science*, 246(4926), 116.

Greene, R.V. & Freer, S.N., 1986. Growth characteristics of a novel nitrogen-fixing cellulolytic bacterium. *Applied and Environmental Microbiology*, 52(5), 982.

Greene, R.V., Cotta, M.A. & Griffin, H.L., 1989. A novel, symbiotic bacterium isolated from marine shipworm secretes proteolytic activity. *Current Microbiology*, 19(6), 353-356.

Griffin, H.L., Freer, S.N. & Greene, R.V., 1987. Extracellular endoglucanase activity by a novel bacterium isolated from marine shipworm. *Biochemical and Biophysical Research Communications*, 144(1), 143–151.

Guerinot, M.L., 1994. Microbial iron transport. *Annual Reviews in Microbiology*, 48(1), 743–772.

Hahnhagerdal, B. et al., 2006. Bio-ethanol – the fuel of tomorrow from the residues of

today. *Trends in Biotechnology*, 24(12), 549-556.

Hall, T., 1999. BioEdit: a user-friendly biological sequence alignment editor and analysis program for Windows 95/98/NT. *Nucleic acids research*, 41, 95-98.

Hammel, K.E., 1997. Fungal degradation of lignin. *Driven by nature: plant litter quality and decomposition. CAB International, Wallingford*, 33–46.

Harvey, A.L., 2008. Natural products in drug discovery. *Drug discovery today*, 13(19-20), 894–901.

Harwood, C., 1990. *Molecular biological methods for Bacillus*, Chichester ;;New York: Wiley.

Haygood, M.G. & Davidson, S.K., 1997. Small-subunit rRNA genes and in situ hybridization with oligonucleotides specific for the bacterial symbionts in the larvae of the bryozoan Bugula neritina and proposal of" Candidatus endobugula sertula". *Applied and environmental microbiology*, 63(11), 4612.

Hernandez, J., 2004. Three fur homologues from Anabaena sp. PCC7120: exploring reciprocal protein-promoter recognition. *FEMS Microbiology Letters*, 236(2), 275-282.

Hibbing, M.E. et al., 2009. Bacterial competition: surviving and thriving in the microbial jungle. *Nature Reviews Microbiology*.

Hostettmann, K., 1998. Strategy for the biological and chemical evaluation of plant extracts. *Pure Appl Chem*, 70(11).

Ikeda, H. et al., 2003. Complete genome sequence and comparative analysis of the industrial microorganism Streptomyces avermitilis. *Nature biotechnology*, 21(5), 526–531.

Imam, S.H., Greene, R.V. & Griffin, H.L., 1990. Adhesive properties of a symbiotic bacterium from a wood-boring marine shipworm. *Applied and Environmental Microbiology*, 56(5), 1317.

Imam, S.H., Greene, R.V. & Griffin, H.L., 1993. Binding of extracellular carboxymethylcellulase activity from the marine shipworm bacterium to insoluble cellulosic substrates. *Applied and Environmental Microbiology*, 59(5), 1259.

Inaba, K. & Oda, T., 1975. Phosphorylation of purine and pyrimidine nucleosides by isolated rat liver mitochondria. *Acta Medica Okayama*, 29(5), 367-375.

Innis, M., 1990. *PCR protocols : a guide to methods and applications*, San Diego: Academic Press.

Institute of Malacology & University of Michigan. Museum of Zoology. Mollusk Division, 1981. Malacologia. Available at: http://www.archive.org/details/malacologia208081inst [Accessed March 9, 2010].

Jenkinson, H.F., Sawyer, W.D. & Mandelstam, J., 1981. Synthesis and order of assembly of spore coat proteins in Bacillus subtilis. *Microbiology*, 123(1), 1.

Kapur, S. & Khosla, C., 2008. Biochemistry: Fit for an enzyme. *Nature*, 454, 832–833.

Keller, A. et al., 2002. Empirical statistical model to estimate the accuracy of peptide identifications made by MS/MS and database search. *Analytical Chemistry*, 74(20), 5383-5392.

Kester, D.R. et al., 1967. Preparation of artificial seawater. *Limnology and Oceanography*, 12(1), 176–179.

Ketley, J.M., 1999. Campylobacter jejuni Contains Two Fur Homologs: Characterization of Iron-Responsive Regulation of Peroxide Stress Defense Genes by the PerR Repressor.

King, A.J. et al., 2010. Molecular insight into lignocellulose digestion by a marine isopod in the absence of gut microbes. *Proceedings of the National Academy of Sciences*. Available at: http://www.pnas.org/cgi/doi/10.1073/pnas.0914228107.

Koumoutsi, A. et al., 2004. Structural and functional characterization of gene clusters directing nonribosomal synthesis of bioactive cyclic lipopeptides in Bacillus amyloliquefaciens strain FZB42. *Journal of bacteriology*, 186(4), 1084.

Kumar, S. et al., 2008. MEGA: a biologist-centric software for evolutionary analysis of DNA and protein sequences. *Briefings in bioinformatics*.

Langman, L. et al., 1972. Enterochelin system of iron transport in Escherichia coli: mutations affecting ferric-enterochelin esterase. *Journal of Bacteriology*, 112(3), 1142.

Lautru, S. et al., 2007a. MbtH-like protein-mediated cross-talk between non-ribosomal peptide antibiotic and siderophore biosynthetic pathways in Streptomyces coelicolor M145. *Microbiology*, 153(5), 1405.

Lautru, S. et al., 2007b. MbtH-like protein-mediated cross-talk between non-ribosomal peptide antibiotic and siderophore biosynthetic pathways in Streptomyces coelicolor M145. *Microbiology*, 153(5), 1405.

Lechene, C.P. et al., 2007. Quantitative Imaging of Nitrogen Fixation by Individual Bacteria Within Animal Cells. *Science*, 317(5844), 1563-1566.

Lee, R.W. & Childress, J.J., 1994. Assimilation of inorganic nitrogen by marine invertebrates and their chemoautotrophic and methanotrophic symbionts. *Applied and Environmental Microbiology*, 60(6), 1852.

Leonowicz, A., 1999. Biodegradation of Lignin by White Rot Fungi. *Fungal Genetics and Biology*, 27(2-3), 175-185.

Letoffe, S., Delepelaire, P. & Wandersman, C., 2004. Free and hemophore-bound heme acquisitions through the outer membrane receptor HasR have different requirements for the TonB-ExbB-ExbD complex. *Journal of bacteriology*, 186(13), 4067.

Lewin, M. & Goldstein, I.S., 1991. International fiber science and technology series, v. 11. *International fiber science and technology series, v. 11*. Available at: http://www.bcin.ca/Interface/openbcin.cgi?submit=submit&Chinkey=127812 [Accessed March 8, 2010].

Lim, G.E. & Haygood, M.G., 2004. "Candidatus Endobugula glebosa," a Specific Bacterial Symbiont of the Marine Bryozoan Bugula simplex. *Applied and Environmental Microbiology*, 70(8), 4921-4929.

Liras, P., Asturias, J. & Martin, J., 1990. Phosphate control sequences involved in transcriptional regulation of antibiotic biosynthesis. *Trends in Biotechnology*, 8, 184-189.

Litwin, C.M., Boyko, S.A. & Calderwood, S.B., 1992. Cloning, sequencing, and transcriptional regulation of the Vibrio cholerae fur gene. *Journal of bacteriology*, 174(6), 1897.

Livak, K., 2001. Analysis of Relative Gene Expression Data Using Real-Time Quantitative PCR and the 2−ΔΔCT Method. *Methods*, 25(4), 402-408.

Loomis, L.D. & Raymond, K.N., 1991. Solution equilibria of enterobactin and metal-enterobactin complexes. *Inorganic Chemistry*, 30(5), 906–911.

Lopes, S.G.B.C. et al., 2000. Functional anatomy of the digestive system of Neoteredo reynei (Bartsch, 1920) and Psiloteredo healdi (Bartsch, 1931) (Bivalvia: Teredinidae). *Geological Society, London, Special Publications*, 177(1), 257-271.

Luo, Y. et al., 2008. Complete genome of Phenylobacterium zucineum–a novel facultative intracellular bacterium isolated from human erythroleukemia cell line K562. *BMC genomics*, 9(1), 386.

Luyten, Y.A. et al., 2006a. Extensive variation in intracellular symbiont community composition among members of a single population of the wood-boring bivalve

Lyrodus pedicellatus (Bivalvia: Teredinidae). *Applied and Environmental Microbiology*, 72(1), 412.

Luyten, Y.A. et al., 2006b. Extensive variation in intracellular symbiont community composition among members of a single population of the wood-boring bivalve Lyrodus pedicellatus (Bivalvia: Teredinidae). *Applied and Environmental Microbiology*, 72(1), 412.

Maplestone, R.A., Stone, M.J. & Williams, D.H., 1992. The evolutionary role of secondary metabolites–a review* 1. *Gene*, 115(1-2), 151–157.

Martin, J.F., 2004. Phosphate control of the biosynthesis of antibiotics and other secondary metabolites is mediated by the PhoR-PhoP system: an unfinished story. *Journal of bacteriology*, 186(16), 5197.

Martin, F.A. et al., 2009. Interplay between Two RND Systems Mediating Antimicrobial Resistance in Brucella suis. *Journal of Bacteriology*, 191(8), 2530-2540.

Martin, J., Casqueiro, J. & Liras, P., 2005. Secretion systems for secondary metabolites: how producer cells send out messages of intercellular communication. *Current Opinion in Microbiology*, 8(3), 282-293.

McHugh, J.P., 2003. Global Iron-dependent Gene Regulation in Escherichia coli: A new mechanism for iron homeostasis. *Journal of Biological Chemistry*, 278(32), 29478-29486.

Miller, M.J. et al., 2009. Utilization of microbial iron assimilation processes for the development of new antibiotics and inspiration for the design of new anticancer agents. *Biometals*, 22(1), 61–75.

Miron, M. et al., 2006. A methodology for global validation of microarray experiments. *BMC bioinformatics*, 7(1), 333.

Moeck, G.S. & Coulton, J.W., 1998. TonB-dependent iron acquisition: mechanisms of siderophore-mediated active transport. *Molecular Microbiology*, 28(4), 675-681.

Moldenhauer, J. et al., 2010. The Final Steps of Bacillaene Biosynthesis in Bacillus amyloliquefaciens FZB42: Direct Evidence for b,g Dehydration by a trans-Acyltransferase Polyketide Synthase. *Angewandte Chemie International Edition*.

Monari, S., 2009. Phylogeny and biogeography of pholadid bivalve Barnea (Anchomasa) with considerations on the phylogeny of Pholadoidea. *Acta Palaeontologica Polonica*, 54(2), 315-335.

Morton, B., 1970. The Functional Anatomy of the Organs of Feeding and Digestion of

Teredo Navalis Linnaeus and *Lyrodus Pedicellatus* (Quatrefages). *Journal of Molluscan Studies*, 39(2-3), 151-167.

Naka, H., López, C.S. & Crosa, J.H., 2008. Reactivation of the vanchrobactin siderophore system of Vibrio anguillarum by removal of a chromosomal insertion sequence originated in plasmid pJM1 encoding the anguibactin siderophore system. *Environmental Microbiology*, 10(1), 265–277.

Neilands, J.B., 1995. Siderophores: structure and function of microbial iron transport compounds. *Journal of Biological Chemistry*, 270(45), 26723.

Nesvizhskii, A.I. et al., 2003. A statistical model for identifying proteins by tandem mass spectrometry. *Analytical Chemistry-Washington DC-*, 75(17), 4646–4658.

Ohkuma, M., 2003. Termite symbiotic systems: efficient bio-recycling of lignocellulose. *Applied microbiology and biotechnology*, 61(1), 1–9.

Oviedo, C. & Rodriguez, J., 2003. EDTA: The chelating agent under environmental scrutiny. *Quimica Nova*, 26, 901–905.

Page, G.P. et al., 2006. The PowerAtlas: a power and sample size atlas for microarray experimental design and research. *BMC bioinformatics*, 7(1), 84.

Patzer, S.I. & Braun, V., 2009. Gene Cluster Involved in the Biosynthesis of Griseobactin, a Catechol-Peptide Siderophore of Streptomyces sp. ATCC 700974. *Journal of Bacteriology*, 192(2), 426-435.

Petersen, D. et al., 2005. Three microarray platforms: an analysis of their concordance in profiling gene expression. *BMC genomics*, 6(1), 63.

Peterson, S., 2004. Multilocus DNA sequence analysis shows that Penicillium biourgeianum is a distinct species closely related to P. brevicompactum and P. olsonii. *Mycological Research*, 108(4), 434-440.

Piel, J., 2004. Metabolites from symbiotic bacteria. *Natural product reports*, 21(4), 519–538.

Pohl, E. et al., 2003. Architecture of a protein central to iron homeostasis: crystal structure and spectroscopic analysis of the ferric uptake regulator. *Molecular Microbiology*, 47(4), 903-915.

Posey, J.E., 2000. Lack of a Role for Iron in the Lyme Disease Pathogen. *Science*, 288(5471), 1651-1653.

Postle, K. & Kadner, R.J., 2003. Touch and go: tying TonB to transport. *Molecular microbiology*, 49(4), 869–882.

Pukatzki, S. et al., 2006. Identification of a conserved bacterial protein secretion system in Vibrio cholerae using the Dictyostelium host model system. *Proceedings of the National Academy of Sciences*, 103(5), 1528.

Pukatzki, S., McAuley, S.B. & Miyata, S.T., 2009. The type VI secretion system: translocation of effectors and effector-domains. *Current Opinion in Microbiology*, 12(1), 11-17.

Raymond, K.N., Dertz, E.A. & Kim, S.S., 2003. Enterobactin: an archetype for microbial iron transport. *Proceedings of the National Academy of Sciences*, 100(7), 3584.

Rodriguez, E. & McDaniel, R., 2001. Combinatorial biosynthesis of antimicrobials and other natural products. *Current opinion in microbiology*, 4(5), 526–534.

Rondon, M.R., Ballering, K.S. & Thomas, M.G., 2004. Identification and analysis of a siderophore biosynthetic gene cluster from Agrobacterium tumefaciens C58. *Microbiology*, 150(11), 3857.

Roosenberg, I.I. et al., 2000. Studies and syntheses of siderophores, microbial iron chelators, and analogs as potential drug delivery agents. *Current medicinal chemistry*, 7(2), 159–197.

Rubin, E.M., 2008. Genomics of cellulosic biofuels. *Nature*, 454(7206), 841-845.

Schmitt, M.P. & Payne, S.M., 1991. Genetic analysis of the enterobactin gene cluster in Shigella flexneri. *Journal of bacteriology*, 173(2), 816.

Schmitt, M.P. & Payne, S.M., 1988. Genetics and regulation of enterobactin genes in Shigella flexneri. *Journal of bacteriology*, 170(12), 5579.

Schulze, A. & Downward, J., 2001. Navigating gene expression using microarrays-a technology review. *Nature Cell Biology*, 3(8), 190–195.

Schwyn, B. & Neilands, J., 1987. Universal chemical assay for the detection and determination of siderophores. *Analytical Biochemistry*, 160(1), 47-56.

Seviour, R.J. et al., 1992. Production of Pullulan and other Exopolysaccharides by Filamentous Fungi. *Critical Reviews in Biotechnology*, 12(3), 279-298.

Shen, B., 2003. Polyketide biosynthesis beyond the type I, II and III polyketide synthase paradigms. *Current Opinion in Chemical Biology*, 7(2), 285-295.

Shi, J. et al., 2006. Evidence supporting predicted metabolic pathways for Vibrio cholerae: gene expression data and clinical tests. *Nucleic acids research*, 34(8), 2438.

Sipe, A.R., Wilbur, A.E. & Cary, S.C., 2000. Bacterial symbiont transmission in the wood-boring shipworm Bankia setacea (Bivalvia: Teredinidae). *Applied and Environmental Microbiology*, 66(4), 1685.

Sola-Landa, A., Moura, R.S. & Martin, J.F., 2003. The two-component PhoR-PhoP system controls both primary metabolism and secondary metabolite biosynthesis in Streptomyces lividans. *Proceedings of the National Academy of Sciences of the United States of America*, 100(10), 6133.

Southern, E. et al., 1999. Molecular interactions on microarrays. *nature genetics*, 21(1), 5–9.

Stork, M. et al., 2004. Two tonB systems function in iron transport in Vibrio anguillarum, but only one is essential for virulence. *Infection and immunity*, 72(12), 7326.

Taylor, L.E. et al., 2006. Complete Cellulase System in the Marine Bacterium Saccharophagus degradans Strain 2-40T. *Journal of Bacteriology*, 188(11), 3849-3861.

Temirov, Y.V. et al., 2003. A Catecholic Siderophore Produced by the Thermoresistant Bacilluslicheniformis VK21 Strain. *Russian Journal of Bioorganic Chemistry*, 29(6), 542–549.

Thompson, J.D., Higgins, D.G. & Gibson, T.J., 1994. CLUSTAL W: improving the sensitivity of progressive multiple sequence alignment through sequence weighting, position-specific gap penalties and weight matrix choice. *Nucleic acids research*, 22(22), 4673.

Tien, M. & Kirk, T.K., 1988. Lignin peroxidase of Phanerochaete chrysosporium. *Methods Enzymol*, 161(23), 238–249.

Toranzo, A.E. et al., 1983. Molecular factors associated with virulence of marine vibrios isolated from striped bass in Chesapeake Bay. *Infection and immunity*, 39(3), 1220.

Touati, D., 2000. Iron and Oxidative Stress in Bacteria. *Archives of Biochemistry and Biophysics*, 373(1), 1-6.

Trindade-Silva, A.E. et al., 2009. Physiological traits of the symbiotic bacterium Teredinibacter turnerae isolated from the mangrove shipworm Neoteredo reynei. *Genetics and Molecular Biology*, 32, 572–581.

Trindade-Silva, A. et al., 2009. Identification of a Putative Catechol-Siderophore Biosynthetic Gene Cluster from the shipworm symbiont, *Teredinibacter turnerae*. In Philippine Mollusk Symbiont ICBG Research Symposium. Oregon Health and

Science University.

Turner, R.D., 1966. *A survey and illustrated catalogue of the Teredinidae (Mollusca: Bivalvia)*, Available at: http://openlibrary.org/b/OL21399459M/survey_and_illustrated_catalogue_of_the_Teredinidae_(mollusca_bivalvia). [Accessed March 12, 2010].

Verbree, E.C., 1995. The Escherichia coli Malonyl-CoA:Acyl Carrier Protein Transacylase at 1.5- Resolution. *Journal of Biological Chemistry*, 270(22), 12961-12964.

Vernon, S.D. et al., 2000. Reproducibility of alternative probe synthesis approaches for gene expression profiling with arrays. *Journal of Molecular Diagnostics*, 2(3), 124.

Wachtershauser, G., 1990. Evolution of the first metabolic cycles. *Proc. Natl. Acad. Sci. USA*, 87(1), 200–204.

Walsh, C.T. et al., 1990. Molecular studies on enzymes in chorismate metabolism and the enterobactin biosynthetic pathway. *Chemical Reviews*, 90(7), 1105-1129.

Wandersman, C. & Stojiljkovic, I., 2000. Bacterial heme sources: the role of heme, hemoprotein receptors and hemophores. *Current opinion in Microbiology*, 3(2), 215–220.

Wang, Y. et al., 2006. Large scale real-time PCR validation on gene expression measurements from two commercial long-oligonucleotide microarrays. *BMC genomics*, 7(1), 59.

Wee, S. et al., 1988. Expression, isolation and properties of Fur (ferric uptake regulation) protein ofEscherichia coli K 12. *Biology of Metals*, 1(1), 62-68.

Weiner, R.M. et al., 2008. Complete Genome Sequence of the Complex Carbohydrate-Degrading Marine Bacterium, Saccharophagus degradans Strain 2-40T W. F. Burkholder, ed. *PLoS Genetics*, 4(5), e1000087.

Winterbourn, C., 1995. Toxicity of iron and hydrogen peroxide: the Fenton reaction. *Toxicology Letters*, 82-83, 969-974.

Xu, P. & Distel, D.L., 2004. Purification and characterization of an endo-1, 4-β-D glucanase from the cellulolytic system of the wood-boring marine mollusk Lyrodus pedicellatus (Bivalvia: Teredinidae). *Marine Biology*, 144(5), 947-953.

Yang, J.C. et al., 2009. The Complete Genome of Teredinibacter turnerae T7901: An Intracellular Endosymbiont of Marine Wood-Boring Bivalves (Shipworms) N. Ahmed, ed. *PLoS ONE*, 4(7), e6085.

Yin, J. et al., 2007. Genome-Wide High-Throughput Mining of Natural-Product Biosynthetic Gene Clusters by Phage Display. *Chemistry & Biology*, 14(3), 303-312.

Zeeck, A., 2001. Enterobactin: the characteristic catecholate siderophore of Enterobacteriaceae is produced by Streptomyces species1. *FEMS Microbiology Letters*, 196, 147–151.

Zhang, S.D. & Gant, T.W., 2004. A statistical framework for the design of microarray experiments and effective detection of differential gene expression. *Bioinformatics*, 20(16), 2821.

Zuccaro, A. et al., 2004. A new Acremonium species associated with Fucus spp., and its affinity with a phylogenetically distinct marine Emericellopsis clade. *Studies in Mycology*, 50, 283–297.

Biographical Sketch

Brian Fishman was born in Buffalo Grove, Illinois on April 7th, 1983. He earned his Bachelor of Science in Biology from Indiana University in 2005, where he was employed in the Chemistry department and performed independent research in the Biology department studying transmission modes of endophytic fungi in local grass populations.

After completing his Bachelor's degree, Brian was employed as a Chemistry Laboratory Associate at Baxter Healthcare Corporation, where he performed quality control for the manufacturing of intravenous antibiotics. In April of 2007, Brian moved to Arizona and was employed at Yulex Corporation as a Research & Development technician, where he developed custom latex medical devices and immunoassays.

Brian moved from Arizona to Portland, Oregon in March of 2008 to begin his graduate work in Dr. Margo Haygood's laboratory at Oregon Health & Science University, which is presented here.